JNC TY8400 2004-001

Interim Report on Research between Oak Ridge National Laboratory and Japan Nuclear Cycle Development Institute on Neutron-Capture Cross Sections by Long-Lived Fission Product Nuclides

(Document on Collaborative Study)

March, 2004

Japan Nuclear Cycle Development Institute
Tokai Works
Oak Ridge National Laboratory

〒319-1184　茨城県那珂郡東海村村松4番地49
核燃料サイクル開発機構
技術展開部　技術協力課
電話：029-282-1122（代表）
ファックス：029-282-7980
電子メール：jserv@jnc.go.jp

JNC TY8400 2004-001

March, 2004

Interim report on research between Oak Ridge National Laboratory and Japan Nuclear Cycle Development Institute on neutron-capture cross sections by Long-Lived Fission Product nuclides

(Document on Collaborative Study)

Kazuyoshi Furutaka[*], Shoji Nakamura[*],
Hideo Harada[*], Subramanian Raman[**,***],
Paul E. Koehler[**]

Abstract

Neutron capture cross sections of long-lived fission products (LLFP) are important quantities as fundamental data for the study of nuclear transmutation of radioactive wastes. Previously obtained thermal-neutron capture gamma-ray data were analyzed to deduce the partial neutron-capture cross sections of LLFPs including ^{99}Tc, ^{93}Zr, and ^{107}Pd for thermal neutrons. By comparing the decay gamma-ray data and prompt gamma-ray data for ^{99}Tc, the relation between the neutron-capture cross section deduced by the two different methods was studied. For the isotopes ^{93}Zr and ^{107}Pd, thermal neutron-capture gamma-ray production cross sections were deduced for the first time. The level schemes of ^{99}Tc, ^{93}Zr, and ^{107}Pd have also been constructed from the analyzed data and compared with previously reported levels.

This work has been done under the cooperative program "Neutron Capture Cross Sections of Long-Lived Fission Products (LLFPs)" by Japan nuclear cycle development institute (JNC) and Oak Ridge National Laboratory (ORNL).

---

[*] Waste Management and Fuel Cycle Research Center, Advanced Fuel Recycle Technology Division, Recycle System Analysis and Design Group
[**] Oak Ridge National Laboratory
[***] Deceased

2004 年 3 月

オークリッジ国立研究所-核燃料サイクル開発機構の長寿命核分裂生成核種の中性子捕獲断面積に関する共同研究中間報告書

（核燃料サイクル開発機構　共同研究報告書）

古高和禎[*]、中村詔司[*]、原田秀郎[*]、
Subramanian Raman[**,***], Paul E. Koehler[**]

要旨

長寿命核分裂生成核種(LLFP)の中性子捕獲断面積は、放射性廃棄物の変換方法の研究の基礎をなす、重要な値である。三核種の LLFP、^{99}Tc、^{93}Zr そして ^{107}Pd の熱中性子捕獲断面積を決定するために、反応で放出される即発ガンマ線の既存の測定データの解析を行った。^{99}Tc に対しては、即発ガンマ線から求めた断面積と崩壊ガンマ線から求めた断面積とを比較した。^{93}Zr と ^{107}Pd に対しては、熱中性子捕獲断面積を初めて実験的に決定した。観測したガンマ線の情報を用い、また既に文献に報告されている情報を活用し、^{99}Tc、^{93}Zr 及び ^{107}Pd の準位図を作成した。

本研究は、核燃料サイクル機構(JNC)と米国オークリッジ国立研究所(ORNL)との間の共同研究「長寿命核分裂生成核種の中性子捕獲断面積に関する共同研究」の下で行った。

[*] 環境保全・研究開発センター　先進リサイクル研究開発部　システム設計評価グループ
[**] Oak Ridge National Laboratory
[***] 逝去

Contents

List of Tables

List of Figures

1 Introduction

Neutron capture cross sections of long-lived fission products (LLFP) are important quantities as fundamental data for the study of nuclear transmutation of radioactive wastes. However, knowledge of their neutron capture cross sections is very limited and the improvement of the data accuracy is an important issue. Japan nuclear cycle development institute (JNC) and Oak Ridge National Laboratory (ORNL) started the program "Neutron Capture Cross Sections of Long-Lived Fission Products (LLFPs)" to improve the accuracy of neutron capture cross section of LLFPs in October 2001. This program is composed of three research items:

1. Analysis of thermal-neutron capture gamma-ray data of LLFPs,
2. Preparation of LLFP samples, and
3. keV neutron capture cross section measurement of LLFPs.

In item 1, previously obtained thermal-neutron capture gamma-ray data were analyzed to deduce the partial neutron-capture cross sections of LLFPs including ^{99}Tc, ^{93}Zr, and ^{107}Pd for thermal neutrons. Information on thermal-neutron capture gamma-ray data is very valuable to deduce the thermal neutron-capture cross sections for ^{93}Zr and ^{107}Pd because the capture products are stable, and hence the conventional activation method cannot be applied. On the other hand, both activation and prompt neutron-capture gamma-ray spectroscopic methods can be, in principle, used for the measurement of the thermal neutron-capture cross section of ^{99}Tc. Therefore, we compared the thermal neutron capture cross section of ^{99}Tc deduced by the activation method to the cross section determined using the prompt neutron-capture gamma-ray spectroscopic method to check the consistency

of the data deduced by the two different methods. For the isotopes ^{93}Zr and ^{107}Pd, thermal neutron-capture gamma-ray production cross sections were deduced for the first time. The level schemes of ^{99}Tc, ^{93}Zr, and ^{107}Pd have also constructed from the analyzed data and compared with previously reported levels. In this report, analytical methods and analyzed data on research item 1 are described. Details on the research of ^{99}Tc were described in chapter 2, these of ^{93}Zr in chapter 3, and these of ^{107}Pd in chapter 4. Summary was given in chapter 5.

2 Research on ^{99}Tc(n_{th},γ) cross section from analysis of prompt γ rays

2.1 Background

The nuclide ^{99}Tc, with a half-life of 2.1×10^5 years [3], is one of the LLFP nuclides which are produced in conventional nuclear power plants with relatively large yields. The nuclide ^{100}Tc, which is produced in neutron capture reaction by ^{99}Tc, β-decays to its stable daughter nuclide ^{100}Ru, with sufficiently short half-life of 15.8 s [3]. This fact, together with its high geochemical mobility, makes the nuclide ^{99}Tc among the possible candidates for transmutation using neutrons. Therefore, accurate ^{99}Tc(n,γ) cross sections are needed to design transmutation systems.

Among neutron cross sections, the one at thermal energy (2200 m/s) is important, because not only is it used by itself but also it is often used to normalize cross section data in the resonance region. Between 1950 to 1970, several authors reported ^{99}Tc(n_{th},γ) cross sections [4–7], ranging from 16 to 24.8 b. A recent value 22.9 ± 1.3 b reported in 1995 by Harada *et al.* [8] is the most precise one. The values reported in the above references as well as the evaluated cross sections are summarized in table 1.

In a series of studies, which have shown that a simple direct reaction mechanism is predominant in the absolute cross sections of primary electric-dipole $E1$ transitions in neutron-capture reactions by light nuclei ($A < 50$) at off-resonance energies [2,9–17], one of the present authors have demonstrated the capabilities of determining the cross sections of the neutron capture reactions, by measuring gamma-ray transitions in singles measurements with a sensitive detection system and constructing level schemes. For heavier nuclei such as ^{99}Tc, which have larger level densities, the situation may not be

that simple: in order to construct level schemes and deduce accurate cross sections of capture reactions for these nuclei, a measurement of gamma-ray energies and intensities may not be sufficient and an examination of coincidence relationships between gamma rays may be needed.

The purposes of the present research were, to analyze the existing data of prompt gamma rays emitted in the thermal neutron capture reaction by ^{99}Tc observed in singles measurements and to obtain a detailed list of the gamma-ray emission cross sections in the reaction as a first step to determine the cross section. From the list of the prompt gamma rays, one can construct the decay scheme of ^{100}Tc and obtain a preliminary value of the cross section. In the present work, the decay gamma rays in ^{100}Ru were also examined to obtain the reaction cross section. During the course of the present study, a brief report of a study along the same line has been published [18].

2.2 Experimental procedures

The (n, γ) measurements were carried out with a 84.6-mg 100 % pure Tc metal target obtained from Petten. The target was studied in the thermal column of the internal target facility at the Los Alamos Omega West Reactor (fig. 1). The target was placed in a graphite holder, which was inside an evacuated bismuth channel. The target position was 1.5 m from the edge of the reactor core. At this position, the thermal neutron flux was $\sim 6 \times 10^{11} n/\mathrm{cm}^2/\mathrm{s}$ and the Cd(In) ratio was ≈ 2000. The Los Alamos facility and the data analysis procedures have been described in detail in Ref. [2]. Gamma-ray spectra were obtained with a 30-cm^3 coaxial intrinsic Ge detector positioned inside a 20-cm-diam by 30-cm-long NaI(Tl) annulus. This Ge detector was located 6.3 m from the target and was operated either in the Compton-suppressed mode (0.388 keV/channel) or in the pair-spectrometer

mode (0.629 keV/channel). The latter mode utilizes the lengthwise optical division of the annulus so that only double-escape peaks appear in the pulse-height spectrum. At lower energies the two annulus halves are connected together electrically to operate in the conventional Compton-suppressed mode. The pulse-height analyzer had 16384 channels. In the Compton-suppressed mode, the full width at half maximum (fwhm) values for our system were 1.5, 1.8, 2.3, and 2.9 keV, respectively, for γ-ray energies of 0.5, 1.0, 2.0, and 3.0 MeV. Figure 2 shows a sample spectrum obtained with the ^{99}Tc target in this mode. In the pair-spectrometer mode, the fwhm values were 2.5, 3.3, 4.0, and 4.7 keV, respectively, for γ-ray energies of 3, 5, 7, and 9 MeV. Figure 3 shows a sample spectrum obtained with the ^{99}Tc target in the latter mode.

Energy calibrations in the pair-spectrometer mode were performed with the prompt γ-ray spectrum from neutron capture in melamine ($C_3H_6N_6$). In the Compton-suppressed mode, the prompt γ ray from the $^1H(n,\gamma)$ reaction plus the annihilation radiation were employed for this purpose. In both modes, nonlinearity corrections to the measured energies were made (see fig. 2 of Ref. [17]), using precisely known γ rays appropriate to the range of energies of interest. The primary calibration energies were those recommended by Wapstra [19,20]: 510.999 ± 0.001 keV for the annihilation radiation, 2223.255 ± 0.003 keV for the γ ray from the $^1H(n,\gamma)$ reaction, and 4945.302 ± 0.003 keV for the ground-state transition in the $^{12}C(n,\gamma)$ reaction. Secondary calibration energies were provided by the γ rays in the $^{14}N(n,\gamma)$ reaction [17].

Intensity calibrations (see fig. 3 of Ref. [17]) were determined in the Compton-suppressed mode with a set of standard radioisotopic sources with precalibrated γ-ray intensities. The efficiency curve in the pair-spectrometer

mode was derived from the relative intensities of γ rays from the $^{14}N(n,\gamma)$ reaction [17, 21]. The effect of possible variations in neutron flux was taken into account by normalizing the data to the neutron fluence for each run measured with a small fission counter located near the target position in the thermal column. The gamma-ray emission cross section reported in the current work is based on measurements in which the target was studied together with a 100.0-mg CH_2 standard. The cross section is normalized to the recommended value of $\sigma_\gamma(2200\ \mathrm{m/s}) = 332.6 \pm 0.7$ mb [22] for ^1H present in the standard. The thermal-neutron flux at the target position approximates a Maxwellian distribution corresponding to a temperature of 350 K, for which the most probable neutron velocity is 2400 m/s. To determine the cross sections at 2200 m/s, we have assumed a $1/v$ dependence of the capture cross section for ^1H and for ^{99}Tc.

2.3 Analyses of measured γ rays

The data obtained in the Compton-suppressed mode and the pair-spectrometer mode were analyzed separately. The analyses of the gamma-ray peaks were done using a program named `skg7`, which is a version of the "SKEWGAUS" program [23]. The areal count of each gamma peak was determined by doing a fit to several peaks (≤ 8) in a given region simultaneously.

The determined areal counts were then corrected for detection efficiencies, and converted to emission cross sections by using the above-mentioned standards, using another program called "`prelvl7`".

The obtained lists of gamma rays which record energies as well as emission cross sections in the Compton-suppressed mode and the pair-spectrometer mode, are then compared and combined into a single list.

From the list, gamma rays which are known to originate from the nuclides

other than ^{100}Tc were then removed by using the existing compilations of gamma rays emitted in neutron capture reactions such as Ref. [24, 25].

The observed gamma rays in the thermal neutron capture reaction by ^{99}Tc are listed in table 2.

The ^{99}Tc(n, γ) reaction with thermal neutrons has been studied previously with Ge detector at the Washington State University reactor by Tarr [26]. The author used a 35-cc Ge(Li) detector and observed a total of 30 gamma rays ranging from 23.97 keV to 6563.4 keV. From the observed gamma rays, the author has constructed a level scheme of ^{100}Tc nuclide, which consist of 21 levels from -6563.6 keV to -4433.2 keV relative to the capture state.

The same reaction has also been extensively studied by Heck and Pinston [27] and by Pinston *et al.* [28]. They have measured gamma rays and conversion electrons emitted in the reaction using a bent-crystal spectrometer, a β spectrometer and various Ge(Li) and Si(Li) detectors, at the Grenoble reactor, the Karlsruhe research reactor, and the Jülich reactor. The report by Heck and Pinston [27] lists the tables of observed gamma rays, and the resultant level scheme is shown in Ref. [28].

2.4 Discussion

From the obtained information on the prompt gamma rays emitted in ^{99}Tc$(n_{\rm th}, \gamma)^{100}$Tc reaction, one can construct the decay scheme of ^{100}Tc and determine the reaction cross section. Also, from the yields of decay gamma rays emitted after the β decay of ^{100}Tc to ^{100}Ru, the cross section can be obtained.

2.4.1 Cross section from prompt gamma rays

To deduce the reaction cross section from intensities of prompt gamma rays, one has first to construct the decay scheme.

To construct the decay scheme from information obtained through singles measurements of prompt gamma rays, a skeleton level scheme was built based on the previously published data.

Previous measurements and skeleton level scheme of ^{100}Tc Table 3 lists the variety of previous measurements that have been carried out concerning the energy levels in ^{100}Tc.

There were several studies which aimed at establishing low-lying levels in ^{100}Tc using ^{99}Tc$(n_{\rm th},\gamma)$ [26, 28], ^{100}Mo$(d,2n\gamma)$ [28], ^{99}Tc(d,p) [29], ^{100}Mo$(p,n\gamma)$ [30–32], and ^{96}Zr(^{7}Li,$3n\gamma$) [33] reactions.

Pinston *et al.* have used the ^{100}Mo$(d,2n\gamma)^{100}$Tc reaction study [28] to investigate isomeric transitions in ms region using a 12-MeV deuteron beam supplied by the Grenoble variable energy cyclotron.

Through the ^{99}Tc$(d,p)^{100}$Tc reaction at $E_d = 15$ MeV, Slater and Booth constructed a level scheme of up to an excitation energy of 1.000 MeV, which consisted of 28 levels including the ground state. From DWBA analyses of the obtained angular distributions, they assigned orbital angular momentum ℓ (and spin-parity J^π if $\ell = 0$) to each level.

One of the three ^{100}Mo$(p,n\gamma)$ studies that of [30] focused on investigating two isomeric transitions and identified an isomeric level with a half-life of 8.46 ± 0.05 μs at an excitation energy of 200.83 ± 0.10 keV. Bini *et al.* [32] investigated low-lying levels of ^{100}Tc with the same reaction in the energy range of $4.0 \leq E_p \leq 6.8$ MeV by means of γ-γ coincidence technique, and constructed a level scheme up to 521.0 keV. Similarly, Árvay *et al.* [31] re-

ported a level scheme of up to 906.1 keV.

High-spin yrast states of ^{100}Tc were investigated using the ^{96}Zr(^{7}Li,3$n\gamma$) reaction [33]. The highest excitation energy and spin reported in the study are 3075.7 keV and 14^{-}, respectively.

From these references we assembled a list (see table 4) of $\sim$ 65 levels in ^{100}Tc below 6.77 MeV. We specifically excluded previous (n,γ) studies. The construction of this skeleton level scheme was nontrivial because it was necessary to establish a one-to-one correspondence between the levels reported in different experiments. Some of these works contain additional information leading to J^{π} values for several levels. We have critically evaluated this information; our adopted J^{π} values are also listed in table 4. Our summary is independent of similar summary appearing in the *Nuclear Data Sheets* [34]. The ^{100}Mo$(p,n\gamma)^{100}$Tc studies by Árvay *et al.* [31] and Bini *et al.* [32] are the backbone of the skeleton level scheme.

Level scheme The problem of constructing a level scheme based on (n,γ) data is rendered easier to the extent to which the energy levels and their branching ratios are known from other experiments. Each known level which could reasonably be expected to receive population in the (n,γ) reaction was checked against the γ-ray data. In this paper, the level scheme of ^{100}Tc based on our (n,γ) study is presented in tabular form in table 5. Less than 8 % of the observed γ rays have been incorporated into this scheme consisting of 36 bound levels.

The level energies listed in this table was obtained through an overall least-squares fit involving all placed transitions. In deducing these level energies, nuclear recoil was taken into account. Also presented in this table is the summed cross section for populating each level, the summed cross sec-

tion for deexciting each level, and the intensity imbalance. The level scheme based on our (n, γ) work is compared to previous work in Table 4.

Neutron separation energy The neutron separation energy was determined to be $S_n(^{100}\mathrm{Tc}) = 6765.20 \pm 0.04$ keV, by performing a least-square fit to energies of primary and secondary gamma rays. The values obtained by Pinston *et al.* [28] ($S_n = 6764.4 \pm 1.0$ keV) and by Slater and Booth [29] ($S_n = 6780 \pm 20$ keV) are consistent with our value. These values are considerably higher than the value listed in Ref. [35] (6600 ± 60 keV). In Ref. [26], it was attempted to determine S_n precisely by assuming that the highest-energy transition observed (6564-keV gamma ray) populates a low-lying state and that the transition from this state to the ground state was also observed. Based on the value of S_n listed in Ref. [35] the author of Ref. [26] searched for a single transition with an energy around 26 keV but could not find (In Ref. [26], the author cited the value of S_n from Ref. [35] as 6590 ± 60 keV). The authors of Ref. [29] suggested that the discrepancy between the value obtained in their study and the one listed in Ref. [35] to the possibility that the accepted value of the endpoint energy [36] for the β^- transition from the ground state of ^{100}Tc to the ground state of ^{100}Ru is overestimated by about 170 keV.

Cross section from ground-state transitions of ^{100}Tc The cross section σ of a neutron capture reaction can be obtained using the following relation:

$$\sigma = \sum_{i=g.s.trans.} (1 + \alpha_{\mathrm{T}}(i)) \times I_\gamma(i), \qquad (1)$$

where the sum runs through all the ground-state transitions, and $\alpha_{\mathrm{T}}(i)$ stand for total internal conversion coefficient for the i-th ground-state transition,

and $I_\gamma(i)$ emission cross section of the gamma ray.

In the present study, six gamma rays have been assigned as ground-state transitions, namely, 172.21, 223.48, 263.58, 340.99, 355.67, and 458.7-keV gamma rays. From information on these gamma rays, the capture cross section can also be determined if the internal conversion coefficients (ICCs) are known. The level scheme obtained in the present work is, however, apparently not complete, and the cross section obtained in this way should be regarded as a lower limit or a proof of the order of magnitude of the values obtained in other methods.

The ICCs of the transitions in ^{100}Tc have been measured and reported for some lower shells by several authors [28, 31, 33]. In order to deduce the capture cross section, however total ICCs were in need, and therefore, these were calculated theoretically using the reported ICCs to the lower shells in the following manner. At first, for each study, the reported values were compared to the theoretical values based on Ref. [37] and the mixing ratios were deduced. If ICCs for several different shells were reported to a transition, a weighted average was taken over the resultant mixing ratios. Then, from the obtained mixing ratio, a total conversion coefficient was calculated using a code HSICC [38]; i.e. calculations of ICCs for K-, L-, and M-shells were based on Ref. [37], for outer shells on Ref. [39], and then ICCs for N- and O-shells were multiplied by 0.975, to give better agreement with the experimental data, as proposed in Ref. [40]. Finally, by taking a weighted average over obtained total ICCs calculated from ICCs for lower shells reported in the previous studies, total conversion coefficients were obtained and are summarized in table 6.

From the information on the six ground-state transitions and the conversion coefficients in table 6, the capture cross section was calculated to be

21.37 ± 0.62 b, where the error includes uncertainties of gamma-ray emission cross sections as well as those of total internal conversion coefficients. Corrections of the internal conversion for 340.99, 355.67, and 458.7 keV gamma rays have not been done because the multipolarities of these gamma rays are not known: if $E2$ is assumed for the 340.99 and 355.67-keV gammas and $M4$ for 458.7-keV one, the correction would amount to less than 0.003 b, far smaller than the uncertainty in the cross section.

Cross section from $\sum E_\gamma I_\gamma / S_n$ If we had observed all the gamma rays from the reaction, then the cross section could be calculated from the relation

$$\sigma = \sum E_\gamma I_\gamma / S_n. \tag{2}$$

Moreover, if we had observed all the gamma rays from the reaction and could construct a complete level scheme, then the cross section could be obtained from the following relation

$$\sigma = \sum I_\gamma(\text{primary}). \tag{3}$$

We can estimate the cross section by using the above relations and the present data.

From the gamma-ray data listed in table 2, we can easily calculate the value of $\sum E_\gamma I_\gamma$. The value obtained is 44591 ± 177 keV·b, which together with $S_n = 6765.20 \pm 0.04$ keV imply $\sigma = 6.59$ b. The low-energy transitions below the detection threshold of the gamma rays in the present experiment, namely 31.3696- and 28.49-keV transitions [27], contribute only an additional 1.67mb. Even after making corrections for conversion electrons for some of lower energy transitions, $\sum E_\gamma I_\gamma$ amounts only to 44998 kev·b, which corre-

sponds to σ = 6.65 b: this is only about 31 % of the value obtained from the relation (1). An estimate of $\sum E_\gamma I_\gamma$ from the data obtained by using the anti-Compton spectrometer and the pair spectrometer in Ref. [27] yields a roughly same value, 51353 keV·b.

Though we did not completely assign all observed gamma rays to the level scheme, we can estimate the cross section by assuming all observed γ rays are primary and hence including all of them with energies below S_n in the summation. Shown in figure 4 is the behavior of the sum when the lower limit of summation was varied. The figure indicates that in order to obtain a cross section of about 20 b, the sum must include gamma rays as low as 300 keV.

These two facts suggest that we did not observe all the gamma rays emitted in the reaction, and illustrates the difficulty in determining the neutron capture cross sections from $\sum E_\gamma I_\gamma / S_n$ and $\sum I_\gamma$ (primary).

2.4.2 Cross section from the decay gamma rays

In the present study, the most accurate and reliable value of the neutron capture cross section was obtained from the gamma rays emitted after β decay of the reaction product ^{100}Tc. The ^{100}Tc nuclide β decays to ^{100}Ru with a half-life of 15.27±0.05 s [41]. After the decay, a few gamma rays are emitted, the most intense ones having energies of 539.34 ± 0.08 keV and 590.61 ± 0.08 keV and emission probabilities as reported in Ref. [41]. In the present study, these two gamma rays were observed at 539.51 ± 0.03 and 590.73 ± 0.03 keV. But according to Ref. [27], there exists another decay gamma ray with an energy of 540.3049 keV. With the resolution of the spectrometer used in the present study, it can not be resolved from the one of 539.34 keV, so a correction must be made. To estimate and subtract the contribution of

the 540.3049-keV gamma ray to the 539.51 keV one, ratios were calculated of the gamma-ray emission cross sections obtained in the present study to that reported in Ref. [27] with the curved-crystal spectrometer, for gamma rays with energies between 470.6 and 610.4 keV having sections larger than 50 mb. In this way, the cross section due to the 540.3049-keV gamma ray was estimated to be 55.62 ± 0.36 mb. The various cross sections are summarized in table 7.

2.4.3 Thermal neutron capture cross section of ^{99}Tc

In the present study, the thermal-neutron capture cross section of ^{99}Tc was determined in two methods; from the prompt gamma rays emitted from the neutron-capture reactions (Eq. 1) and from the gamma rays following the beta decay of the reaction product. The values obtained were 21.37 ± 0.62 b, and 22.8 ± 1.8 b, for the two methods respectively. Even though the obtained level scheme is not complete, the value obtained in the former method amounted to $\sim$ 94 % of the one in the latter. Of the capture cross section obtained using equation (1), $\sim$ 99 % comes from that of the three lowest ground-state transitions, namely 172.21-, 223.48-, and 263.58-keV gamma rays. This fact suggest that, it is efficient to determine the cross section by observing ground-state transitions in precision singles as well as coincidence measurements.

2.5 Summary and Conclusions

In the present report, we have studied the primary and secondary γ rays from ^{100}Tc following thermal-neutron capture on ^{99}Tc. By incorporating the prompt γ rays into a level scheme which included two newly found levels, six gamma rays were confirmed to be ground-state transitions of ^{100}Tc. From the

sum of the intensities of these six gamma rays, a lower-limit for the neutron capture reaction of 21.37 ± 0.62 b was obtained. This value agrees within the uncertainties with the cross section obtained from the intensities of gamma rays of the activation product ^{100}Ru, 22.8 ± 1.8 b. The reaction cross section obtained from the intensities and the energies of the observed prompt gamma rays amounted only to 6.65 b. This fact suggests that there remain many high-energy gamma rays which were too weak to be observed.

Table 1: Summary of ^{99}Tc thermal neutron capture cross section reported previously.

Author(s)	Cross section (b)	Reference (Year)
Pattenden *et al.*	24.8 ± 2.0	[4] (1958)
Tattersall *et al.*	16 ± 7	[42] (1960)
Ovechkin *et al.*	24 ± 2	[6] (1974)
Pomerance	19 ± 2	[43] (1975)
Lucas *et al.*	20 ± 2	[7] (1977)
Harada *et al.*	22.9 ± 1.3	[8] (1995)
Molnár *et al.*	24.3 ± 1.8 (decay γ)	[18] (2002)
	21.21 ± 0.17 (prompt γ, lower limit)	
ENDF/B-VI	19.5	[44] (1993)
JENDL-3.2	19.641	[45] (1995)
JENDL-3.3	22.77	[46] (2002)

Table 2: Energies (E_γ) and intensities (I_γ) of γ rays from the ^{99}Tc(n_{th},γ)^{100}Tc reaction.

E_γ (keV)[a]	I_γ (mb)[a]	E_γ (keV)[a]	I_γ (mb)[a]	E_γ (keV)[a]	I_γ (mb)[a]
30.8 *6*	102 *12*	140.34 *5*	90 *4*	236.47 *5*	36.6 *20*
39.12 *5*	87 *5*	141.49 *10*	32 *3*	238.66 *11*	35 *4*
43.18 *3*	269 *7*	144.27 *3*	196 *5*	239.52 *4*	91 *4*
45.84 *8*	38 *4*	145.73 *5*	58 *3*	244.68 *12*	21 *3*
50.85 *9*	3.1 *4*	152.74 *3*	78.7 *11*	247.15 *16*	16 *2*
51.70 *9*	3.8 *4*	159.22 *3*	48.3 *18*	252.26 *3*	332 *7*
52.85 *6*	6.1 *4*	160.81 *18*	4.5 *12*	253.56 *5*	96 *4*
53.71 *10*	3.1 *4*	163.12 *5*	29.5 *22*	257.46 *6*	51 *3*
56.63 *6*	7.1 *6*	166.58 *6*	355 *29*	260.97 *3*	139 *4*
62.79 *3*	399 *11*	168.87 *8*	503 *46*	263.58 *3*	1453 *17*
63.75 *4*	186 *8*	169.95 *18*	258 *39*	269.15 *13*	38 *6*
71.62 *6*	32 *2*	172.21 *3*	16694 *536*	270.04 *4*	150 *6*
73.11 *8*	22.4 *24*	176.51 *4*	29.4 *16*	274.83 *22*	14 *2*
75.02 *8*	105 *21*	179.77 *9*	52 *8*	276.55 *3*	849 *10*
75.52 *3*	364 *22*	180.36 *4*	112 *8*	280.48 *8*	10.3 *10*
76.9 *5*	13.0 *21*	182.98 *21*	4.7 *16*	281.98 *3*	57.9 *12*
86.76 *4*	457 *30*	185.67 *3*	57.3 *12*	283.21 *9*	10.8 *10*
90.59 *3*	308 *42*	190.70 *3*	37.9 *10*	285.03 *7*	10.9 *9*
91.32 *3*	1177 *77*	194.44 *4*	58 *2*	286.83 *3*	31.2 *11*
94.58 *5*	3.7 *3*	196.47 *3*	464 *6*	288.74 *3*	80.3 *14*
99.02 *3*	129 *2*	199.3 *4*	13 *6*	291.20 *14*	22 *4*
102.85 *13*	19 *2*	199.98 *11*	44 *6*	292.94 *4*	98 *4*
103.80 *10*	31 *3*	202.9 *5*	9 *5*	295.43 *4*	94 *4*
105.43 *8*	337 *86*	203.7 *8*	6 *5*	297.10 *7*	62 *3*
105.81 *6*	436 *87*	206.17 *3*	302 *6*	299.48 *3*	3095 *40*
107.25 *15*	15 *2*	209.64 *6*	47 *3*	300.92 *7*	591 *31*
109.9 *7*	2.4 *24*	211.31 *5*	76 *4*	301.65 *15*	129 *37*
113.20 *3*	115 *3*	213.24 *3*	517 *8*	304.83 *7*	25.2 *18*
115.86 *14*	6.5 *13*	217.17 *3*	439 *9*	306.09 *12*	13.3 *17*
118.93 *3*	30.4 *13*	220.18 *3*	206 *6*	308.74 *3*	70.3 *18*
124.66 *11*	8.9 *12*	221.87 *5*	132 *7*	312.30 *3*	74.8 *23*
127.47 *4*	88 *6*	223.48 *3*	1511 *23*	313.45 *9*	24.8 *20*
128.08 *12*	35 *6*	225.38 *3*	656 *18*	317.48 *20*	74 *16*
129.24 *7*	20.8 *16*	226.42 *4*	304 *14*	318.39 *20*	72 *16*
132.88 *9*	5.0 *6*	230.25 *3*	93 *3*	321.58 *6*	144 *9*
134.84 *25*	1.7 *7*	231.35 *6*	46 *2*	323.78 *6*	149 *9*
139.05 *11*	27 *3*	233.22 *10*	16.5 *20*	327.45 *17*	10.6 *21*

Table 2: (*continued*)

E_γ (keV)[a]	I_γ (mb)[a]	E_γ (keV)[a]	I_γ (mb)[a]	E_γ (keV)[a]	I_γ (mb)[a]
329.43 *3*	67.0 *24*	419.97 *23*	10.7 *21*	514.93 *3*	81.0 *23*
332.41 *13*	13.5 *19*	421.73 *6*	50 *2*	516.73 *9*	15.1 *24*
335.29 *4*	47.1 *22*	423.78 *8*	34.7 *23*	518.42 *5*	12.2 *6*
338.95 *3*	661 *7*	426.10 *8*	31.5 *23*	520.62 *7*	26 *2*
340.99 *3*	152 *3*	429.54 *5*	148 *8*	523.34 *3*	167 *3*
344.89 *3*	250 *5*	430.50 *12*	56 *7*	528.42 *13*	11.10 *15*
346.36 *17*	153 *60*	433.45 *6*	47.2 *25*	531.85 *10*	15.5 *16*
346.83 *20*	113 *61*	437.55 *4*	20.9 *9*	536.67 *6*	44 *7*
348.89 *3*	166 *3*	439.43 *5*	21.1 *9*	544.32 *5*	98 *4*
352.00 *7*	28.7 *24*	440.71 *14*	7.0 *9*	545.41 *14*	42 *4*
355.67 *4*	47.4 *19*	443.60 *7*	9.7 *7*	546.97 *10*	41 *2*
357.37 *4*	111 *4*	445.66 *8*	8.4 *7*	548.29 *18*	16.4 *24*
358.31 *5*	70 *3*	448.06 *4*	18.1 *8*	550.96 *3*	77.5 *21*
360.49 *8*	17.2 *16*	452.87 *4*	53.8 *23*	552.78 *10*	21.5 *18*
363.32 *12*	13.3 *19*	454.81 *8*	30.0 *21*	555.01 *4*	50.2 *20*
364.84 *6*	32.3 *18*	456.99 *3*	89 *2*	558.20 *4*	49.5 *23*
366.32 *3*	60.7 *18*	458.7 *3*	39.8 *23*	562.34 *4*	49.1 *18*
370.42 *3*	60.6 *9*	460.40 *4*	75 *2*	565.21 *3*	59.6 *17*
372.33 *5*	14.9 *8*	463.69 *3*	162 *3*	568.04 *3*	71.4 *19*
374.32 *4*	17.10 *10*	465.95 *11*	20.0 *21*	569.97 *3*	98.7 *20*
376.10 *8*	10.5 *12*	470.64 *3*	265 *5*	574.37 *4*	58.2 *19*
378.01 *10*	24 *3*	472.1 *4*	14 *3*	576.06 *19*	10.4 *17*
379.61 *8*	32 *3*	473.5 *6*	18 *8*	578.43 *14*	21 *2*
381.86 *4*	69 *3*	474.4 *6*	20 *7*	579.60 *13*	22 *2*
385.00 *3*	289 *4*	475.61 *17*	33 *4*	583.28 *3*	65.4 *15*
386.62 *4*	93 *3*	479.41 *9*	36 *2*	588.27 *7*	35.5 *19*
390.04 *3*	241 *4*	480.91 *9*	41 *2*	593.89 *6*	42.8 *18*
393.07 *4*	76 *3*	482.46 *17*	19 *2*	595.55 *22*	10.1 *18*
396.00 *5*	60 *2*	484.43 *3*	166 *3*	597.07 *13*	19.1 *19*
398.00 *5*	142 *6*	486.45 *4*	78 *2*	599.15 *14*	14.5 *18*
399.17 *3*	275 *7*	488.79 *3*	73 *2*	601.06 *18*	10.6 *19*
401.50 *3*	99 *3*	491.30 *5*	42 *2*	604.85 *5*	35.5 *18*
404.53 *25*	5.9 *15*	493.76 *9*	15.8 *17*	607.71 *8*	19.5 *15*
405.91 *13*	11.5 *14*	495.90 *9*	33 *2*	610.53 *7*	25.4 *15*
409.32 *19*	6.1 *11*	496.99 *14*	25 *2*	614.39 *3*	71.6 *19*
411.20 *6*	20.5 *12*	498.50 *4*	47.6 *17*	619.06 *3*	60.5 *16*
413.83 *3*	131.4 *19*	503.32 *3*	78.1 *15*	621.46 *6*	71 *4*

Table 2: (*continued*)

E_γ (keV)[a]	I_γ (mb)[a]	E_γ (keV)[a]	I_γ (mb)[a]	E_γ (keV)[a]	I_γ (mb)[a]
622.43 *8*	54 *4*	719.39 *14*	30.1 *20*	828.75 *11*	20.10 *18*
625.97 *9*	16.7 *12*	720.53 *7*	34.1 *24*	830.05 *12*	19.4 *19*
628.72 *5*	30.3 *13*	723.37 *4*	26.10 *9*	832.62 *7*	30.0 *14*
633.91 *3*	44.8 *15*	725.46 *18*	6.2 *9*	834.21 *15*	16.2 *14*
636.55 *6*	15.4 *15*	727.53 *16*	12.8 *18*	835.88 *15*	11.5 *13*
639.41 *5*	44.3 *16*	728.70 *9*	23.6 *17*	839.71 *16*	9.8 *12*
640.69 *12*	18.1 *16*	732.5 *4*	4.3 *17*	840.86 *10*	15.1 *13*
642.56 *9*	30.8 *22*	736.86 *4*	51.9 *20*	847.27 *5*	30.10 *11*
643.64 *17*	14.3 *22*	739.44 *12*	15.8 *25*	849.87 *6*	23.1 *10*
648.25 *5*	54.10 *20*	741.74 *15*	8.1 *15*	852.43 *4*	39.2 *12*
649.44 *18*	15.2 *19*	743.88 *5*	24.7 *13*	855.10 *10*	13.5 *12*
651.12 *4*	40.5 *13*	746.45 *3*	44.3 *12*	859.01 *14*	19.7 *22*
653.10 *3*	57.4 *13*	749.56 *4*	33.3 *14*	860.14 *21*	11.2 *24*
657.46 *3*	31.6 *9*	752.06 *10*	12.0 *17*	862.89 *4*	30.9 *11*
660.67 *7*	12.7 *8*	754.38 *7*	43 *2*	866.77 *21*	7.7 *13*
663.17 *6*	17.4 *8*	756.52 *4*	67 *2*	868.34 *8*	28.3 *15*
665.06 *6*	36.4 *14*	760.13 *12*	18.5 *21*	870.04 *18*	10.4 *16*
666.34 *3*	78.1 *15*	764.14 *10*	11.2 *11*	872.58 *11*	28.3 *24*
668.60 *3*	34.9 *9*	767.57 *7*	33 *2*	873.88 *21*	29 *2*
670.49 *15*	6.8 *9*	768.64 *9*	32 *2*	874.97 *12*	30 *3*
673.47 *14*	8.0 *14*	771.17 *10*	11.3 *9*	878.68 *19*	7.7 *14*
678.70 *3*	39.5 *8*	774.25 *8*	14.3 *11*	881.05 *6*	24.3 *13*
681.42 *5*	23.7 *9*	781.01 *13*	21.7 *19*	886.36 *6*	24.7 *13*
682.88 *3*	86.2 *10*	782.66 *21*	12.9 *17*	888.79 *21*	7.4 *16*
684.75 *12*	7.4 *7*	785.48 *16*	11.10 *16*	892.77 *11*	18.6 *18*
687.86 *3*	9.7 *11*	790.44 *5*	22.9 *14*	893.96 *13*	16.2 *17*
689.88 *8*	29.4 *21*	794.77 *4*	34.4 *11*	899.90 *11*	17.2 *16*
691.06 *19*	19.1 *17*	799.55 *5*	23.10 *11*	904.36 *10*	24.6 *16*
692.32 *12*	17.4 *17*	802.73 *20*	8.5 *12*	906.73 *11*	19.10 *16*
695.58 *18*	7.3 *17*	804.30 *14*	19.9 *15*	912.19 *8*	18.1 *11*
697.73 *10*	13.3 *14*	805.73 *10*	23.9 *15*	914.44 *23*	5.6 *10*
700.41 *8*	17.6 *12*	807.85 *13*	10.7 *13*	917.21 *12*	13.2 *10*
703.88 *3*	94.1 *18*	810.29 *9*	19.8 *24*	919.07 *7*	23.1 *11*
705.38 *10*	21.4 *16*	813.40 *3*	201 *2*	923.30 *23*	6.8 *16*
710.32 *11*	11.9 *11*	815.02 *20*	14.5 *20*	926.01 *3*	62.4 *15*
712.99 *5*	27.9 *11*	818.52 *4*	28.6 *11*	928.57 *13*	11.8 *12*
718.15 *16*	14.3 *18*	825.90 *18*	6.8 *17*	935.51 *11*	13.2 *11*

Table 2: (*continued*)

E_γ (keV)[a]	I_γ (mb)[a]	E_γ (keV)[a]	I_γ (mb)[a]	E_γ (keV)[a]	I_γ (mb)[a]
938.61 *10*	17.1 *11*	1052.51 *4*	28.4 *9*	1158.5 *3*	5.0 *10*
940.63 *12*	13.5 *11*	1055.18 *8*	15.6 *10*	1162.34 *4*	36.8 *10*
943.69 *4*	45.4 *12*	1061.80 *5*	25.7 *9*	1164.92 *15*	4.3 *10*
946.70 *5*	29.8 *12*	1064.68 *8*	15.4 *9*	1167.76 *18*	6.0 *9*
950.09 *12*	14.10 *13*	1067.09 *5*	31.5 *10*	1170.69 *10*	11.1 *11*
952.08 *16*	14.9 *14*	1069.42 *7*	19.3 *10*	1174.37 *5*	23.2 *10*
953.84 *18*	11.6 *14*	1072.06 *5*	23.1 *12*	1180.69 *4*	33.2 *9*
958.23 *3*	45.2 *13*	1074.87 *15*	7.8 *14*	1186.2 *3*	5.6 *11*
962.31 *9*	16.3 *11*	1076.96 *15*	7.7 *15*	1187.54 *14*	10.8 *12*
965.94 *8*	18.1 *11*	1079.70 *5*	23.10 *13*	1190.44 *17*	5.2 *6*
968.62 *3*	55.9 *12*	1082.98 *7*	17.5 *10*	1192.89 *3*	43.3 *7*
971.97 *4*	43.7 *12*	1085.33 *7*	18.3 *10*	1197.20 *25*	4.7 *10*
976.65 *13*	22.1 *23*	1088.18 *9*	12.4 *12*	1201.39 *4*	24.1 *10*
977.9 *3*	10.8 *22*	1091.34 *7*	20.6 *15*	1205.11 *7*	24.4 *10*
982.8 *3*	11.5 *22*	1094.57 *18*	15.9 *22*	1207.07 *14*	11.2 *10*
984.31 *9*	43.1 *23*	1095.9 *3*	16.1 *19*	1210.61 *15*	13.2 *12*
986.26 *12*	20.8 *16*	1097.45 *18*	14.1 *16*	1212.3 *3*	8.9 *11*
989.09 *13*	14.7 *16*	1105.53 *5*	46.2 *15*	1214.47 *13*	14.4 *9*
994.93 *5*	30.7 *12*	1108.56 *18*	16.10 *19*	1216.76 *4*	40.7 *10*
998.43 *13*	14.3 *12*	1110.34 *19*	26.3 *23*	1223.8 *3*	4.7 *8*
1000.34 *14*	14.9 *12*	1112.03 *9*	52.4 *24*	1230.0 *3*	8.3 *19*
1002.48 *10*	16.3 *11*	1113.9 *3*	10.8 *19*	1231.4 *3*	9.8 *19*
1005.9 *3*	5.5 *11*	1117.54 *14*	5.10 *10*	1234.96 *11*	14.8 *10*
1008.82 *24*	7.10 *13*	1120.95 *5*	20.8 *8*	1237.01 *12*	16.9 *10*
1010.66 *7*	29.0 *14*	1123.73 *8*	14.5 *8*	1239.19 *23*	7.0 *10*
1017.42 *19*	9.1 *11*	1125.62 *12*	10.2 *8*	1245.23 *7*	27.3 *15*
1019.14 *12*	14.9 *11*	1128.78 *9*	12.8 *9*	1252.84 *18*	10.9 *17*
1024.48 *7*	17.3 *9*	1130.71 *21*	5.8 *10*	1257.9 *3*	15 *3*
1028.20 *14*	8.10 *10*	1134.35 *12*	12.1 *11*	1271.2 *17*	3 *3*
1032.9 *3*	6.6 *12*	1136.18 *5*	30.4 *11*	1276.58 *23*	6.5 *10*
1034.40 *7*	24.3 *13*	1139.54 *4*	26.3 *9*	1278.90 *7*	20.8 *9*
1037.06 *7*	19.5 *9*	1142.85 *6*	23.7 *9*	1283.7 *4*	3.10 *10*
1038.96 *19*	9.7 *10*	1144.85 *15*	8.9 *9*	1286.06 *13*	11.9 *11*
1040.86 *7*	39.3 *14*	1148.23 *4*	27.7 *11*	1293.36 *3*	91.8 *11*
1042.35 *13*	15.4 *14*	1150.64 *11*	10.4 *13*	1299.53 *5*	31.0 *9*
1045.52 *3*	45.2 *13*	1153.61 *3*	29.2 *9*	1301.98 *20*	7.5 *8*
1049.32 *11*	10.3 *10*	1156.60 *12*	9.4 *9*	1304.79 *12*	11.4 *8*

Table 2: (*continued*)

E_γ (keV)[a]	I_γ (mb)[a]	E_γ (keV)[a]	I_γ (mb)[a]	E_γ (keV)[a]	I_γ (mb)[a]
1308.91 *14*	13.8 *11*	1438.85 *6*	20.5 *8*	1631.4 *3*	6.3 *9*
1310.7 *4*	5.2 *11*	1443.20 *15*	7.9 *8*	1634.26 *14*	11.7 *9*
1313.48 *13*	10.5 *10*	1447.17 *8*	15.5 *8*	1644.52 *18*	8.6 *8*
1317.38 *17*	7.3 *11*	1451.2 *4*	4.6 *10*	1648.1 *3*	5.6 *8*
1325.28 *5*	36.6 *11*	1453.1 *3*	5.1 *10*	1652.4 *3*	4.7 *8*
1328.37 *11*	15.10 *10*	1458.12 *13*	10.7 *8*	1657.47 *8*	20.1 *9*
1330.94 *22*	7.8 *10*	1460.15 *19*	7.2 *8*	1670.03 *15*	10.3 *9*
1335.00 *16*	9.3 *12*	1467.36 *6*	22.4 *11*	1678.3 *3*	3.9 *9*
1340.06 *21*	8.9 *12*	1471.34 *11*	11.8 *9*	1693.6 *3*	5.6 *9*
1342.40 *11*	18.3 *12*	1475.7 *3*	3.10 *10*	1699.4 *4*	3.6 *9*
1344.81 *19*	13.5 *15*	1479.19 *9*	14.10 *11*	1704.0 *3*	6.0 *9*
1346.68 *24*	10.5 *15*	1482.59 *19*	7.3 *14*	1710.81 *8*	24.3 *11*
1352.90 *12*	11.3 *10*	1487.12 *14*	13.5 *13*	1713.73 *15*	12.10 *10*
1357.32 *14*	12.5 *10*	1497.67 *14*	8.4 *9*	1723.53 *24*	9.5 *12*
1359.6 *3*	6.4 *10*	1502.48 *17*	6.8 *8*	1726.1 *4*	5.3 *11*
1362.14 *14*	3.1 *17*	1505.97 *10*	12.8 *8*	1731.9 *3*	5.4 *10*
1363.83 *21*	14.4 *15*	1512.14 *3*	11 *4*	1739.7 *5*	3.7 *10*
1366.27 *22*	8.3 *12*	1519.50 *18*	8.0 *11*	1745.58 *22*	8.6 *10*
1370.83 *15*	8.9 *11*	1522.8 *4*	3.3 *10*	1757.75 *19*	8.1 *9*
1373.67 *11*	14.9 *9*	1532.2 *5*	2.10 *8*	1760.50 *23*	6.5 *9*
1375.68 *10*	16.6 *10*	1536.0 *3*	4.5 *9*	1764.79 *19*	6.9 *8*
1380.48 *10*	11.9 *10*	1542.32 *24*	6.5 *9*	1769.9 *3*	5.4 *8*
1383.25 *11*	11.0 *9*	1544.42 *16*	10.6 *9*	1772.8 *4*	3.6 *8*
1386.01 *5*	27.7 *8*	1547.04 *19*	8.4 *8*	1778.94 *11*	13.8 *8*
1388.78 *11*	11.10 *8*	1549.25 *15*	9.10 *8*	1782.3 *3*	4.4 *8*
1391.40 *13*	11.1 *9*	1552.9 *3*	3.7 *7*	1786.35 *23*	6.0 *9*
1393.62 *14*	10.3 *9*	1559.3 *4*	1.3 *7*	1791.8 *3*	4.8 *9*
1399.73 *19*	5.8 *8*	1564.33 *20*	5.5 *7*	1803.9 *3*	5.1 *9*
1403.35 *8*	14.3 *7*	1570.32 *12*	14.1 *11*	1809.36 *15*	11.4 *11*
1408.12 *12*	9.5 *7*	1576.69 *16*	9.7 *10*	1812.2 *3*	4.5 *10*
1412.2 *3*	4.4 *8*	1582.5 *5*	2.7 *8*	1815.7 *3*	4.8 *9*
1414.9 *4*	3.3 *9*	1587.9 *3*	4.6 *8*	1819.5 *3*	6.3 *11*
1419.77 *15*	11.2 *12*	1596.8 *7*	2.3 *10*	1821.55 *25*	9.2 *11*
1424.6 *6*	6 *2*	1602.34 *17*	9.8 *10*	1824.6 *3*	6.3 *10*
1425.9 *5*	8 *2*	1606.60 *21*	7.9 *9*	1827.09 *23*	7.1 *10*
1430.91 *10*	13.1 *8*	1612.0 *3*	4.9 *9*	1834.9 *3*	5.6 *9*
1434.11 *12*	10.2 *8*	1618.05 *13*	13.4 *10*	1838.5 *3*	4.5 *8*

Table 2: (*continued*)

E_γ (keV)[a]	I_γ (mb)[a]	E_γ (keV)[a]	I_γ (mb)[a]	E_γ (keV)[a]	I_γ (mb)[a]
1842.0 *4*	5.1 *9*	2070.0 *8*	2.3 *9*	2329.7 *3*	5.10 *8*
1844.50 *20*	10.1 *10*	2077.6 *3*	7.1 *10*	2332.8 *6*	3.9 *9*
1847.61 *16*	4.0 *11*	2087.2 *4*	4.2 *9*	2335.9 *5*	4.0 *8*
1854.59 *24*	7.6 *11*	2090.03 *20*	9.3 *9*	2340.5 *3*	6.5 *8*
1859.20 *21*	9.3 *11*	2092.89 *13*	12.6 *8*	2344.6 *3*	5.2 *8*
1862.7 *5*	4.2 *11*	2097.0 *3*	5.4 *7*	2352.7 *4*	3.9 *9*
1867.6 *5*	4.6 *12*	2099.84 *19*	7.9 *7*	2362.4 *3*	6.2 *10*
1870.1 *3*	7.2 *12*	2116.9 *4*	4.9 *10*	2370.7 *3*	7.10 *10*
1874.8 *3*	5.1 *10*	2124.12 *19*	10.4 *11*	2373.8 *5*	4.1 *9*
1877.90 *15*	9.0 *9*	2127.9 *3*	6.6 *11*	2378.48 *19*	10.4 *9*
1884.88 *19*	2.7 *8*	2130.7 *4*	6.4 *11*	2387.8 *3*	6.2 *9*
1891.35 *24*	5.7 *9*	2137.52 *13*	17.2 *11*	2394.43 *19*	10.2 *10*
1896.4 *4*	3.8 *11*	2140.41 *25*	9.2 *11*	2404.92 *21*	8.5 *9*
1902.45 *23*	7.4 *10*	2148.3 *3*	7.7 *11*	2408.1 *3*	7.6 *9*
1909.0 *3*	6.2 *9*	2153.90 *24*	8.2 *10*	2411.31 *24*	7.2 *8*
1916.4 *4*	4.1 *12*	2159.64 *25*	7.9 *10*	2417.0 *3*	6.4 *8*
1924.0 *5*	3.1 *8*	2163.7 *5*	4.3 *11*	2420.9 *7*	2.6 *8*
1930.60 *21*	6.10 *8*	2174.94 *25*	7.7 *10*	2424.4 *3*	6.3 *8*
1939.8 *5*	3.1 *8*	2179.56 *24*	7.9 *10*	2428.09 *17*	9.8 *8*
1946.8 *8*	1.10 *10*	2184.8 *3*	6.9 *9*	2436.3 *4*	5.8 *11*
1953.6 *3*	5.8 *9*	2192.01 *22*	8.5 *10*	2441.5 *4*	4.8 *10*
1960.0 *4*	2.2 *9*	2204.7 *5*	4.7 *11*	2448.0 *3*	5.9 *10*
1965.64 *24*	7.1 *9*	2207.8 *6*	3.5 *11*	2455.9 *4*	4.6 *9*
1974.7 *11*	1.5 *10*	2213.1 *4*	5.2 *13*	2460.5 *5*	4.5 *9*
1982.4 *4*	4.6 *11*	2231.1 *5*	3.8 *11*	2477.28 *14*	14.5 *10*
1986.4 *8*	2.6 *11*	2234.8 *5*	4.1 *10*	2484.4 *3*	8.1 *10*
1991.65 *24*	8.7 *13*	2248.51 *24*	7.5 *9*	2492.2 *4*	5.0 *10*
2006.0 *5*	4.2 *12*	2253.25 *20*	9.1 *9*	2501.1 *3*	4.8 *9*
2013.2 *3*	5.4 *8*	2263.4 *8*	3.2 *11*	2508.41 *15*	11.1 *8*
2022.9 *3*	9.6 *14*	2266.0 *5*	4.5 *11*	2513.5 *5*	3.1 *7*
2025.6 *3*	9.4 *13*	2274.4 *5*	3.10 *10*	2527.37 *25*	7.4 *10*
2032.75 *18*	11.6 *11*	2281.3 *3*	7.6 *9*	2533.2 *4*	4.3 *9*
2046.3 *3*	7.4 *11*	2284.8 *6*	3.5 *9*	2538.13 *23*	7.8 *10*
2048.7 *4*	5.3 *11*	2289.4 *4*	4.8 *9*	2544.7 *3*	7.3 *12*
2057.5 *4*	4.5 *9*	2302.5 *5*	3.6 *10*	2548.1 *3*	6.6 *13*
2062.8 *9*	2.0 *9*	2308.3 *3*	5.8 *9*	2555.23 *24*	6.9 *8*
2066.6 *3*	6.9 *9*	2320.4 *3*	4.8 *8*	2558.45 *16*	10.3 *7*

Table 2: (*continued*)

E_γ (keV)[a]	I_γ (mb)[a]	E_γ (keV)[a]	I_γ (mb)[a]	E_γ (keV)[a]	I_γ (mb)[a]
2566.3 *3*	4.7 *7*	2818.4 *5*	4.2 *11*	3049.0 *3*	6.2 *10*
2569.8 *4*	4.4 *7*	2827.5 *3*	7.6 *10*	3058.6 *3*	9.10 *15*
2574.2 *4*	3.10 *8*	2830.9 *4*	5.9 *10*	3067.06 *11*	12.2 *8*
2590.5 *3*	9.6 *12*	2840.67 *24*	9.3 *10*	3071.5 *3*	5.8 *8*
2593.3 *4*	7.1 *12*	2846.33 *20*	11.5 *10*	3074.43 *14*	12.4 *8*
2604.60 *25*	9.3 *11*	2859.4 *4*	4.9 *11*	3079.96 *11*	13.5 *9*
2609.79 *24*	9.7 *12*	2870.02 *22*	8.3 *9*	3083.66 *17*	8.7 *10*
2617.9 *3*	5.4 *7*	2879.56 *24*	7.6 *8*	3089.13 *13*	13.3 *14*
2621.5 *4*	3.4 *7*	2886.3 *4*	5.3 *8*	3094.8 *3*	8.10 *11*
2631.2 *4*	3.7 *7*	2890.43 *16*	12.4 *9*	3102.6 *3*	8.1 *12*
2641.0 *3*	7.6 *11*	2897.1 *3*	7.4 *9*	3105.7 *3*	8.10 *13*
2644.48 *21*	10.9 *10*	2909.49 *13*	14.1 *8*	3115.53 *25*	9.1 *10*
2650.8 *4*	5.4 *10*	2918.06 *22*	7.9 *8*	3120.48 *22*	12.10 *11*
2661.65 *17*	11.10 *9*	2922.8 *9*	4.4 *19*	3123.9 *5*	6.4 *11*
2671.7 *3*	9.4 *11*	2928.28 *23*	8.7 *9*	3127.2 *4*	6.5 *11*
2674.8 *3*	8.8 *11*	2929.1 *5*	8.2 *20*	3135.0 *3*	7.5 *10*
2694.3 *3*	8.1 *11*	2934.7 *4*	4.2 *8*	3141.8 *7*	7.5 *25*
2697.4 *5*	5.3 *11*	2945.1 *3*	4.5 *9*	3143.90 *23*	7.4 *9*
2709.5 *5*	4.3 *13*	2952.0 *4*	3.8 *9*	3148.1 *5*	8.8 *22*
2713.8 *7*	3.9 *11*	2957.1 *4*	5.3 *8*	3149.3 *3*	7.1 *8*
2717.1 *4*	6.2 *11*	2960.2 *4*	6.1 *8*	3155.55 *9*	18.1 *8*
2722.2 *3*	7.3 *10*	2963.6 *3*	6.0 *7*	3160.51 *20*	8.5 *8*
2732.23 *22*	8.8 *11*	2974.7 *3*	5.7 *8*	3164.4 *6*	7.8 *22*
2745.6 *3*	5.7 *10*	2978.2 *3*	7.1 *9*	3166.55 *16*	10.3 *8*
2757.51 *22*	8.4 *9*	2984.01 *23*	9.0 *9*	3172.72 *13*	19.9 *10*
2761.7 *3*	8.2 *10*	2987.15 *19*	13.8 *10*	3174.83 *3*	16.5 *12*
2764.6 *3*	9.2 *10*	2989.9 *6*	7.4 *12*	3188.4 *6*	7.5 *22*
2768.0 *5*	4.6 *9*	2991.3 *4*	12 *2*	3198.0 *5*	9.7 *22*
2773.58 *19*	11.3 *11*	2992.3 *4*	6.7 *12*	3210.3 *5*	8.9 *22*
2776.65 *20*	11.4 *12*	2998.5 *4*	4.4 *9*	3225.8 *5*	12 *2*
2782.5 *3*	6.6 *8*	3012.67 *16*	11.1 *8*	3233.4 *8*	7 *2*
2786.12 *20*	11.3 *9*	3018.5 *3*	5.9 *8*	3244.2 *4*	15 *2*
2789.2 *3*	6.9 *9*	3024.8 *3*	6.3 *9*	3265.8 *9*	6 *2*
2796.6 *3*	5.8 *8*	3033.2 *3*	8.4 *10*	3270.7 *6*	9 *2*
2800.60 *22*	8.0 *8*	3036.3 *3*	11.8 *11*	3278.9 *3*	12.1 *23*
2807.8 *3*	7.4 *9*	3039.7 *5*	7.2 *11*	3285.1 *4*	10.0 *20*
2811.3 *3*	7.5 *9*	3042.6 *4*	7.1 *11*	3289.0 *6*	6.5 *20*

Table 2: (*continued*)

E_γ (keV)[a]	I_γ (mb)[a]	E_γ (keV)[a]	I_γ (mb)[a]	E_γ (keV)[a]	I_γ (mb)[a]
3302.9 *9*	4.2 *20*	3600.7 *3*	19 *2*	3957.1 *7*	4.8 *16*
3311.6 *6*	11 *3*	3605.6 *4*	14.6 *25*	3969.2 *5*	7.8 *18*
3314.7 *6*	11 *3*	3613.80 *18*	32 *2*	3985.1 *3*	15.0 *20*
3321.6 *6*	9 *3*	3621.79 *23*	20.4 *23*	3998.3 *6*	7.6 *19*
3329.4 *10*	5.6 *25*	3633.2 *9*	5.0 *20*	4009.7 *5*	9.7 *19*
3332.1 *9*	6.1 *24*	3658.2 *5*	8.4 *20*	4014.7 *4*	10.3 *19*
3341.38 *22*	20.0 *22*	3672.1 *11*	5 *3*	4021.1 *4*	10.9 *19*
3347.0 *3*	14.2 *21*	3695.81 *11*	20.3 *12*	4034.7 *3*	16.6 *20*
3360.90 *25*	16.9 *20*	3736.08 *24*	14.0 *18*	4041.60 *21*	22.5 *21*
3367.9 *4*	9.6 *20*	3756.5 *4*	14.7 *25*	4045.7 *3*	14.2 *20*
3379.0 *5*	9.2 *22*	3763.4 *7*	7.2 *24*	4065.61 *16*	21.5 *16*
3381.9 *5*	10.8 *23*	3768.8 *6*	9.1 *24*	4072.00 *14*	25.0 *16*
3395.4 *3*	14.1 *20*	3779.4 *5*	7.2 *18*	4082.94 *22*	15.2 *17*
3401.8 *6*	6.6 *18*	3784.3 *3*	11.5 *18*	4096.3 *3*	21.3 *24*
3407.0 *3*	17.2 *20*	3788.9 *4*	9.2 *18*	4102.3 *4*	12.1 *22*
3410.1 *3*	16.9 *20*	3793.3 *4*	8.7 *18*	4115.4 *3*	15.10 *23*
3419.17 *23*	17.3 *19*	3803.8 *4*	10.9 *18*	4128.82 *25*	10.4 *13*
3426.0 *3*	12.5 *19*	3809.41 *23*	19.4 *19*	4133.61 *24*	10.7 *13*
3440.6 *3*	20 *2*	3812.9 *8*	5.4 *17*	4138.8 *4*	7.3 *13*
3443.8 *4*	15 *2*	3821.3 *5*	7.6 *17*	4143.33 *20*	15.2 *14*
3450.2 *4*	13 *2*	3832.5 *5*	7.9 *17*	4147.01 *19*	16.1 *14*
3453.1 *4*	17 *2*	3836.8 *5*	7.5 *17*	4163.6 *3*	14.7 *18*
3460.6 *21*	3 *2*	3852.1 *5*	7.9 *17*	4167.0 *7*	6.1 *17*
3473.1 *7*	9 *2*	3863.75 *24*	18.7 *20*	4172.3 *4*	8.5 *16*
3476.6 *5*	12 *3*	3876.4 *5*	8.6 *19*	4184.0 *4*	10.7 *19*
3495.1 *9*	5.2 *21*	3881.5 *4*	11.3 *19*	4192.86 *22*	20.7 *21*
3501.2 *6*	7.2 *21*	3886.2 *6*	6.7 *19*	4206.6 *6*	7.4 *19*
3509.9 *3*	15.7 *22*	3891.3 *5*	9.1 *19*	4212.0 *3*	13.10 *20*
3522.7 *6*	9.3 *23*	3904.3 *5*	7.6 *17*	4216.6 *4*	12.8 *19*
3525.8 *5*	10.6 *24*	3909.3 *4*	9.2 *17*	4228.28 *21*	16.9 *17*
3536.4 *3*	9.6 *17*	3915.98 *21*	19.7 *18*	4235.2 *3*	17.2 *19*
3542.6 *4*	7.4 *16*	3920.2 *3*	11.6 *18*	4238.29 *15*	32.5 *20*
3557.2 *4*	8.3 *15*	3927.09 *21*	18.10 *18*	4244.5 *5*	7.4 *15*
3563.0 *4*	8.4 *15*	3932.6 *3*	22 *2*	4248.9 *4*	10.1 *18*
3573.8 *3*	8.9 *15*	3934.9 *6*	9 *2*	4253.3 *3*	11.7 *18*
3586.1 *6*	8.1 *24*	3940.9 *4*	9.3 *20*	4259.1 *3*	12.3 *18*
3591.5 *4*	13.6 *25*	3949.71 *21*	18.7 *18*	4266.95 *10*	45.3 *23*

Table 2: (*continued*)

E_γ (keV)[a]	I_γ (mb)[a]	E_γ (keV)[a]	I_γ (mb)[a]	E_γ (keV)[a]	I_γ (mb)[a]
4272.5 *3*	10.8 *18*	4553.96 *15*	19.9 *14*	4852.8 *3*	9.9 *12*
4282.4 *3*	21.5 *23*	4560.38 *18*	16.0 *13*	4861.1 *5*	10.5 *17*
4285.0 *4*	14.9 *22*	4567.73 *24*	25 *2*	4864.3 *4*	12.4 *17*
4291.2 *3*	14.6 *16*	4570.3 *3*	23.7 *23*	4873.28 *21*	17.8 *15*
4296.7 *4*	8.4 *16*	4573.2 *3*	14.1 *19*	4901.64 *19*	19.10 *15*
4304.1 *3*	11.4 *16*	4586.35 *17*	21.6 *16*	4906.2 *5*	8.4 *13*
4312.84 *24*	15.4 *16*	4592.5 *4*	7.6 *15*	4910.3 *5*	8.1 *13*
4329.8 *3*	8.6 *14*	4600.9 *5*	6.3 *15*	4915.52 *14*	27.4 *16*
4336.74 *16*	19.6 *14*	4607.0 *5*	6.10 *14*	4925.65 *23*	14.9 *16*
4344.2 *5*	5.10 *12*	4618.05 *11*	32.7 *16*	4936.60 *11*	25.9 *13*
4357.93 *12*	27.2 *14*	4626.4 *4*	9.4 *14*	4954.8 *5*	8.10 *21*
4366.3 *3*	10.6 *13*	4630.0 *5*	7.6 *13*	4968.58 *13*	19.8 *12*
4381.70 *22*	14.8 *20*	4637.0 *3*	9.6 *13*	4975.04 *8*	36.1 *13*
4383.69 *16*	27.4 *23*	4641.90 *23*	17.1 *15*	4979.25 *15*	18.9 *11*
4388.8 *4*	6.7 *12*	4645.3 *5*	7.6 *14*	4988.7 *3*	11.3 *11*
4398.9 *3*	10.9 *13*	4653.2 *3*	9.6 *13*	4992.4 *4*	8.8 *12*
4404.26 *14*	21.0 *14*	4658.88 *21*	18.6 *14*	4995.9 *3*	14.8 *13*
4409.5 *3*	11.1 *13*	4662.67 *18*	21.1 *14*	4999.4 *6*	5.7 *12*
4418.59 *18*	16.7 *14*	4670.70 *22*	14.4 *13*	5010.80 *19*	22.0 *17*
4433.85 *20*	32 *2*	4679.0 *3*	18.7 *20*	5015.25 *20*	21.1 *16*
4446.3 *3*	18 *2*	4681.7 *3*	18.3 *21*	5033.40 *16*	24.5 *15*
4455.56 *13*	25.3 *17*	4689.1 *6*	4.7 *12*	5046.81 *18*	20.9 *15*
4462.1 *5*	20 *5*	4700.4 *4*	7.3 *12*	5057.5 *4*	9.6 *14*
4464.00 *19*	62 *5*	4719.9 *4*	16 *3*	5063.84 *15*	26.2 *15*
4467.7 *5*	8.2 *16*	4722.50 *18*	44 *2*	5070.6 *5*	6.5 *13*
4472.68 *15*	22.8 *17*	4729.7 *4*	18 *3*	5094.12 *12*	52 *3*
4480.10 *14*	20.7 *13*	4732.2 *3*	28 *2*	5110.68 *12*	25.8 *13*
4484.81 *21*	13.6 *12*	4740.4 *4*	18 *2*	5120.7 *4*	7.1 *13*
4491.2 *3*	9.2 *12*	4744.2 *3*	21.3 *24*	5129.08 *9*	39.2 *15*
4496.0 *5*	7.8 *15*	4752.62 *18*	27.9 *21*	5139.7 *3*	9.4 *11*
4498.88 *22*	17.10 *15*	4773.50 *18*	21.10 *17*	5153.03 *16*	18.6 *12*
4506.96 *21*	24.1 *20*	4782.6 *3*	11.6 *15*	5168.57 *8*	47.4 *15*
4508.75 *3*	1 *2*	4795.27 *16*	23.4 *16*	5174.6 *3*	10.5 *11*
4511.83 *11*	33.9 *15*	4810.7 *3*	10.6 *12*	5185.5 *3*	9.8 *11*
4522.1 *3*	10.0 *14*	4823.9 *4*	13.9 *19*	5194.1 *3*	9.2 *11*
4539.6 *4*	9.4 *14*	4826.80 *25*	20.9 *19*	5216.05 *7*	30.3 *8*
4543.4 *3*	10.0 *15*	4839.28 *5*	82.3 *22*	5222.09 *12*	14.6 *7*

Table 2: (*continued*)

E_γ (keV)[a]	I_γ (mb)[a]	E_γ (keV)[a]	I_γ (mb)[a]	E_γ (keV)[a]	I_γ (mb)[a]
5229.6 *3*	6.4 *6*	5496.2 *3*	10.2 *10*	5927.0 *3*	6.3 *7*
5241.4 *4*	3.10 *6*	5518.51 *6*	63.7 *16*	5935.45 *13*	17.5 *8*
5245.78 *20*	9.3 *7*	5528.3 *6*	4.5 *9*	5943.25 *9*	25.4 *9*
5254.1 *3*	5.5 *8*	5551.47 *8*	32.8 *11*	5981.13 *23*	6.3 *6*
5258.79 *19*	9.10 *8*	5577.2 *6*	5.10 *11*	6017.4 *6*	1.3 *5*
5265.87 *13*	19.1 *10*	5580.9 *7*	5.10 *11*	6055.64 *20*	9.0 *7*
5269.4 *3*	0.9 *10*	5584.9 *5*	6.7 *10*	6063.7 *4*	3.6 *6*
5285.2 *7*	3.8 *10*	5595.7 *3*	9.6 *11*	6084.13 *24*	5.6 *5*
5290.2 *8*	3.4 *10*	5605.3 *6*	2.9 *7*	6125.16 *13*	15.9 *9*
5297.6 *4*	2.5 *11*	5613.4 *5*	3.8 *7*	6130.46 *19*	9.9 *7*
5306.2 *3*	9.10 *11*	5621.35 *19*	10.3 *8*	6165.09 *18*	9.1 *6*
5319.4 *3*	9.8 *11*	5637.2 *3*	6.4 *7*	6184.47 *17*	10.0 *6*
5324.21 *22*	14.3 *11*	5655.57 *15*	20.5 *12*	6212.7 *4*	3.5 *5*
5340.8 *8*	3.8 *10*	5659.94 *8*	47.2 *16*	6219.97 *5*	58.1 *13*
5344.7 *6*	4.9 *10*	5664.7 *3*	9.9 *9*	6225.17 *12*	17.5 *8*
5351.7 *6*	4.1 *10*	5696.73 *3*	151.10 *24*	6250.85 *14*	12.5 *6*
5371.91 *9*	36.9 *13*	5713.81 *8*	37.1 *12*	6264.74 *8*	29.7 *9*
5383.8 *5*	4.0 *9*	5720.65 *12*	22.9 *11*	6270.6 *6*	7.8 *6*
5389.65 *16*	27.7 *17*	5727.90 *22*	11.4 *10*	6303.91 *25*	7.7 *6*
5392.45 *11*	40.8 *18*	5754.59 *5*	101.9 *21*	6308.5 *4*	4.6 *5*
5401.68 *11*	20.7 *9*	5764.78 *24*	12.10 *12*	6340.3 *8*	1.2 *4*
5411.81 *3*	208.6 *24*	5772.4 *6*	4.7 *11*	6364.5 *4*	2.9 *4*
5420.8 *3*	6.0 *8*	5792.95 *16*	20.2 *12*	6444.9 *4*	2.6 *4*
5434.94 *13*	41.9 *20*	5811.7 *4*	5.2 *8*	6470.2 *4*	2.9 *4*
5437.9 *3*	18.4 *18*	5835.2 *3*	6.7 *8*	6477.2 *3*	3.3 *4*
5452.8 *3*	9.5 *11*	5878.32 *8*	46.6 *14*	6501.1 *3*	3.6 *4*
5457.1 *6*	5.6 *11*	5899.51 *17*	7.6 *5*	6520.5 *6*	1.4 *3*
5460.9 *4*	7.8 *11*	5907.4 *6*	2.2 *5*	6564.26 *10*	17.1 *7*
5468.91 *4*	111.5 *22*	5911.3 *6*	2.5 *5*	6593.2 *8*	1.2 *3*

[a] In our notation, 30.8 *6* $\equiv 30.8 \pm 0.6$, etc.

Table 3: Partial list of references to previous measurements on ^{100}Tc levels.

Measurement	Author(s)	Year	Facility[a]	Reference
^{99}Tc(thermal n,γ) reaction	P. W. Tarr	1972	Washington State U	[25]
	J. A. Pinston *et al.*	1979	Grenoble/Karlsruhe/Jülich	[27]
^{100}Mo($d,2n\gamma$) reaction	J. A. Pinston *et al.*	1979	Grenoble	[27]
^{99}Tc(d,p) reaction	D. N. Slater and W. Booth	1976	U. Oxford	[28]
^{100}Mo($p,n\gamma$) reaction	D. J. Martin and S. A. Wender	1978	McMaster U/Queen's U	[29]
	M. Bini *et al.*	1980	Legnaro	[31]
	Z. Árvay *et al.*	1981	Debrecen	[30]
^{96}Zr(^{7}Li, $3n\gamma$) reaction	A. M. Bizzeti-Sona *et al.*	1995	Legnaro	[32]
^{101}Ru($\gamma,p\gamma$) reaction	H. Bartsch *et al.*	1978	Giessen	[46]
^{99}Tc(res n,γ) reaction	R. L. Macklin	1982	Oak Ridge	[47]
^{100}Mo(^{3}He,t) reaction	H. Akimune *et al.*	1997	RCNP	[48]

[a] Facility where the actual measurements were done. The symbol U stands for a university.

Table 4: Known energy levels in ^{100}Tc deduced from previous work.

Known E (level) (keV)[a]	J^π	Previous (n,γ) E (level) (keV)	This work (n,γ) E (level) (keV)[a]	Known E (level) (keV)[a]	J^π	Previous (n,γ) E (level) (keV)	This work (n,γ) E (level) (keV)[a]
0.0	1^+	0.0	0.0	635.94 *11*	(2–5)		
172.12 *4*	2^+	172.1484	172.205 *23*	639 *10*	$(2–7)^+$	639.805	639.90 *5*
200.43 *4*	4^+	200.6649	200.73 *3*	679.96 *8*	(2–5)		
223.41 *7*	$(0–2)^-$	223.4682	223.48 *3*	689 *10*	$(4^+,5^+)$		
243.8 *4*	$(6)^+$	243.952	243.99 *4*	707.6 *4*	(8^-)		
263.40 *4*	$(3)^+$	263.5558	263.555 *20*	709 *10*	$4^+,5^+$		
287.29 *9*	$(4,5)^+$	287.516	287.58 *3*	710.6 *4*	$(8)^+$		
294.7 *4*	$(4,5)^+$	294.925	295.04 *4*	758 *10*	$4^+,5^+$		
299.61 *7*	$2^+,3^+$		299.68 *5*	758.7 *5*			
319.3 *4*	5^+	319.490	319.59 *4*	776 *10*	$4^+,5^+$		
335.07 *4*	(1–3)		335.26 *5*	777.7 *5*	(9)		
340.97 *5*	$(2,3)^+$	340.979	341.021 *23*	830.20 *7*	$(2,3)^+$		
355.40 *4*	(1–3)		355.67 *4*	854 *10*	$(2–7)^+$		853.97 *15*
400.5 *4*	$(2–7)^+$	400.633	400.78 *5*	882 *10*	$(2–7)^+$		
424.32 *12*	(1–4)	424.359	424.21 *6*	906.11 *8*	(≤ 3)		
440.2 *4*	$(7)^+$			936 *10*	$(2–7)^+$		
454.09 *12*	$(2–5)^+$	454.193	454.24 *3*	950 *10*	$(2–7)^+$		952.77 *5*
456.9 *4*	$(7)^+$			972 *10*	$(2–7)^+$		
459.2 *3*	(≤ 3)		459.03 *4*	1000 *10*	$4^+,5^+$		
460 *10*	$4^+,5^+$	461.096	461.69 *4*	1074.4 *5*	(8^-)		
475.97 *11*	(≤ 3)			1154.7 *5*	(10)		
483.94 *5*	(≤ 3)			1284.5 *5*	$(9)^+$		
493.5 *4*	(2–7)	493.675	493.77 *3*	1400 *100*			
499.88 *5*	(≤ 4)	500.021	500.03 *4*	1406.4 *4*	(11)		
		500.148	500.24 *3*	1720.7 *5*	(10)		
514 *10*	$2^+–7^+$		514.03 *5*	1840.0 *5*	(12)		
521.0 *5*	(1–4)			2175.4 *6*	(11)		
		539.635	539.69 *4*	2238.2 *5*	(13)		
544.7 *4*	6^-	544.875	545.04 *5*	2600 *100*	(1^+)		
552 *10*	$4^+,5^+$	552.280	552.33 *4*	2693.2 *5*	(14)		
		580.415	580.47 *4*	2695.8 *7*	(12)		
600 *10*	$(2–7)^+$		599.96 *6*	3075.7 *7*	(13)		
608.5 *4*	(7)						

[a] In our notation, 172.12 *4* $\equiv 172.12 \pm 0.04$, etc.

Table 5: Level scheme of ^{100}Tc from this work.

E (level) (keV)[a]	J^π	Deexciting γ rays[b]	I_γ (in) (mb)[a]	I_γ (out) (mb)[a]	I_γ (in − out) (mb)[a]
0.0	1^+		19.9 *6*		19.9 *6*
172.206 *23*	2^+	172.21	1.83 *9*	16.7 *6*	−14.9 *6*
200.73 *3*	4^+		5.40 *6*		5.40 *6*
223.48 *3*		223.48	0.866 *11*	1.511 *24*	−0.65 *3*
243.99 *4*	$(6)^+$	43.18	0.365 *22*	0.270 *8*	0.096 *24*
263.555 *20*	$(3)^+$	263.58, 91.32, 62.79	0.453 *14*	3.03 *8*	−2.58 *9*
287.57 *3*	$(4,5)^+$	86.76	1.06 *4*	0.46 *3*	0.61 *5*
295.05 *4*	$(4,5)^+$	94.58, 30.8	0.82 *9*	0.106 *12*	0.71 *9*
299.68 *5*	$2^+,3^+$	127.47		0.088 *7*	−0.088 *7*
319.59 *4*	5^+	118.93, 75.52	0.0026 *4*	0.394 *22*	−0.392 *22*
335.26 *5*	(1–3)	163.12, 71.62		0.062 *4*	−0.062 *4*
341.020 *23*	$(2,3)^+$	340.99, 168.87, 140.34, 76.9, 45.84	0.242 *4*	0.80 *5*	−0.55 *5*
355.67 *4*	(1–3)	355.67		0.0474 *19*	−0.0474 *19*
400.78 *5*	$(2–7)^+$	199.98, 105.81	0.251 *10*	0.48 *9*	−0.23 *9*
424.22 *6*	(1–4)	160.81, 129.24	0.185 *12*	0.0253 *20*	0.160 *12*
454.24 *3*	$(2–5)^+$	253.56, 166.58, 113.20	0.106 *4*	0.57 *3*	−0.46 *3*
456.69 *10*		233.22	0.0046 *6*	0.0165 *20*	−0.0119 *21*
459.03 *4*	(≤3)	458.7, 286.83		0.071 *3*	−0.071 *3*
461.69 *4*	$4^+,5^+$	260.97	0.0077 *7*	0.139 *5*	−0.132 *5*
493.77 *3*	(2–7)	230.25, 206.17, 152.74	0.0078 *6*	0.473 *8*	−0.466 *8*
500.03 *4*	(≤4)	276.55, 236.47		0.886 *11*	−0.886 *11*
500.24 *3*		299.48, 159.22	0.399 *13*	3.14 *5*	−2.74 *5*
514.03 *5*	$2^+–7^+$	313.45, 226.42	0.0125 *7*	0.329 *15*	−0.316 *15*
539.69 *4*		338.95, 244.68	0.0175 *8*	0.682 *8*	−0.665 *8*
545.04 *5*	6^-	144.27	0.0581 *13*	0.196 *6*	−0.138 *6*
552.34 *4*	$4^+,5^+$	288.74, 257.46, 128.08	0.13 *4*	0.166 *8*	−0.03 *4*
580.47 *4*		379.61, 292.94, 179.77	0.0249 *11*	0.182 *11*	−0.157 *11*
599.96 *6*	$(2–7)^+$	145.73	0.0091 *7*	0.058 *4*	−0.049 *4*
639.92 *4*	$(2–7)^+$	127.47		0.088 *7*	−0.088 *7*
747.92 *7*		546.97, 323.78	0.0013 *5*	0.190 *11*	−0.188 *11*
821.80 *6*		321.58	0.0254 *9*	0.144 *10*	−0.118 *10*
853.97 *15*	$(2–7)^+$	301.65	0.0025 *5*	0.13 *4*	−0.13 *4*
929.87 *4*		666.34, 429.54	0.0067 *8*	0.226 *9*	−0.219 *9*
952.77 *5*	$(2–7)^+$	498.50, 372.33	0.0052 *8*	0.0625 *19*	−0.0573 *21*
1051.18 *4*		550.96, 411.20	0.0371 *12*	0.0980 *25*	−0.061 *3*
6765.20[c] *4*	$4^+,5^+$	6593.2, 6564.26, 6520.5, 6501.1, 6477.2, 6470.2, 6340.3, 6308.5, 6303.91, 6270.6,6264.74, 6250.85, 6225.17, 6219.97, 6212.7, 6184.47, 6165.09, 6125.16, 6017.4, 5943.25, 5911.3, 5835.2, 5811.7, 5713.81		0.291 *4*	−0.291 *4*

[a] In our notation, 172.12 *4* ≡ 172.12 ± 0.04, etc.

[b] See also table 4.

[c] Capturing state.

Table 6: Internal Conversion Coefficients

reference	reported multipolarity	conversion coefficients used to calculate α_T	α_T[a]
		172 keV gamma ray	
[28]	$M1+(18 \pm 10)\%E2$	$\alpha_K, \alpha_{L1}, \alpha_M$	0.0834 *8*
[31]	$M1+(12 \pm 7)\%E2$	α_K, α_{L+M}	0.0810 *78*
[33]	$M1$ $(+E2)$	α_K	0.0810 *126*
		weighted average	0.0834 *126*
c.f. Ref. [34]			0.086 *8*
		223 keV gamma ray	
[28]	$E1$	α_K	0.0137 *32*
[31]	$E1+(5 \pm 2)\%M2$	α_K	0.0218 *52*
		weighted average	0.0159 *52*
c.f. Ref. [34]			0.0131
		263 keV gamma ray	
[28]	$E2$	α_K	0.0396 *1*
[33]	$E2$	α_K	0.0420 *73*
		weighted average	0.0396 *73*
c.f. Ref. [34]			0.040

[a] In our notation, 0.0834 *8* $\equiv 0.0834 \pm 0.0008$, etc.

Table 7: Cross sections deduced from the gamma ray emission cross section (I_γ) following the β decay of ^{100}Tc, produced by thermal neutron capture on ^{99}Tc.

E_γ (keV)[a]	I_γ (b)[a]	σ (b)[a]
539.51 *3*	1.550 *10*[b]	23.5 *18*
590.73 *3*	1.232 *8*	22.4 *12*
weighted average		22.8 *18*

[a] In our notation, 539.51 *3* $\equiv 539.51 \pm 0.03$, etc.

[b] After subtraction of contribution from 540.3049-keV gamma ray.

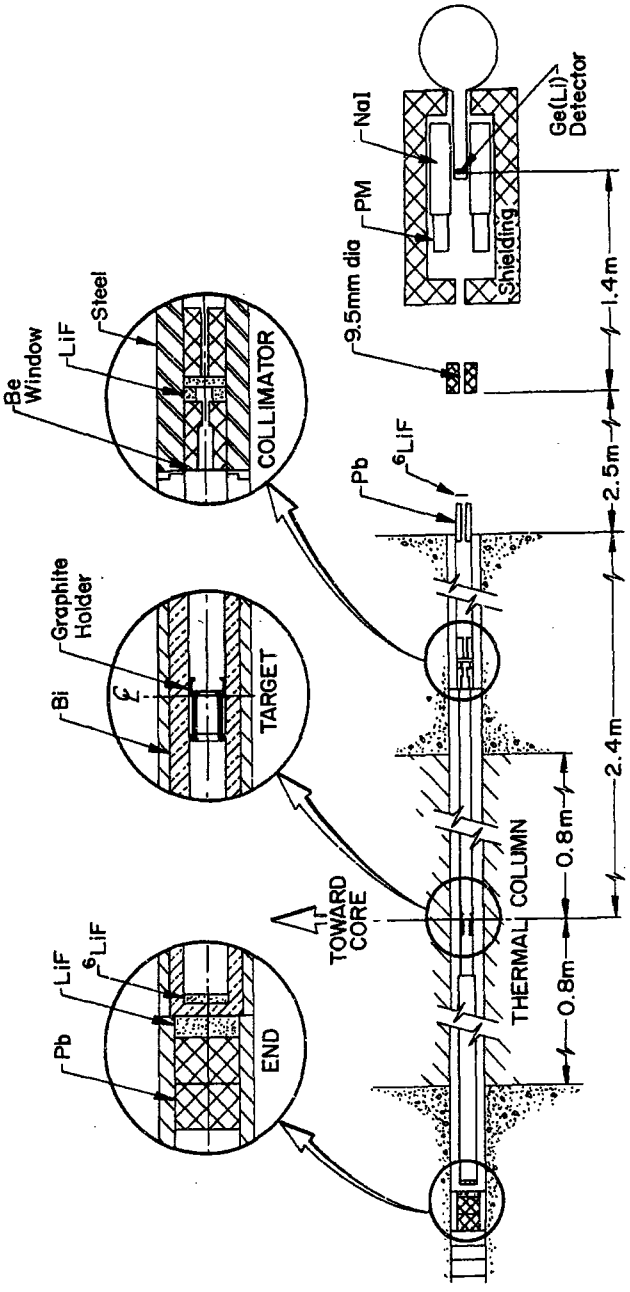

Fig. 1: Experimental arrangement of the target, collimator, and detector at the Los Alamos Omega West Reactor. Excerpted from Ref. [7].

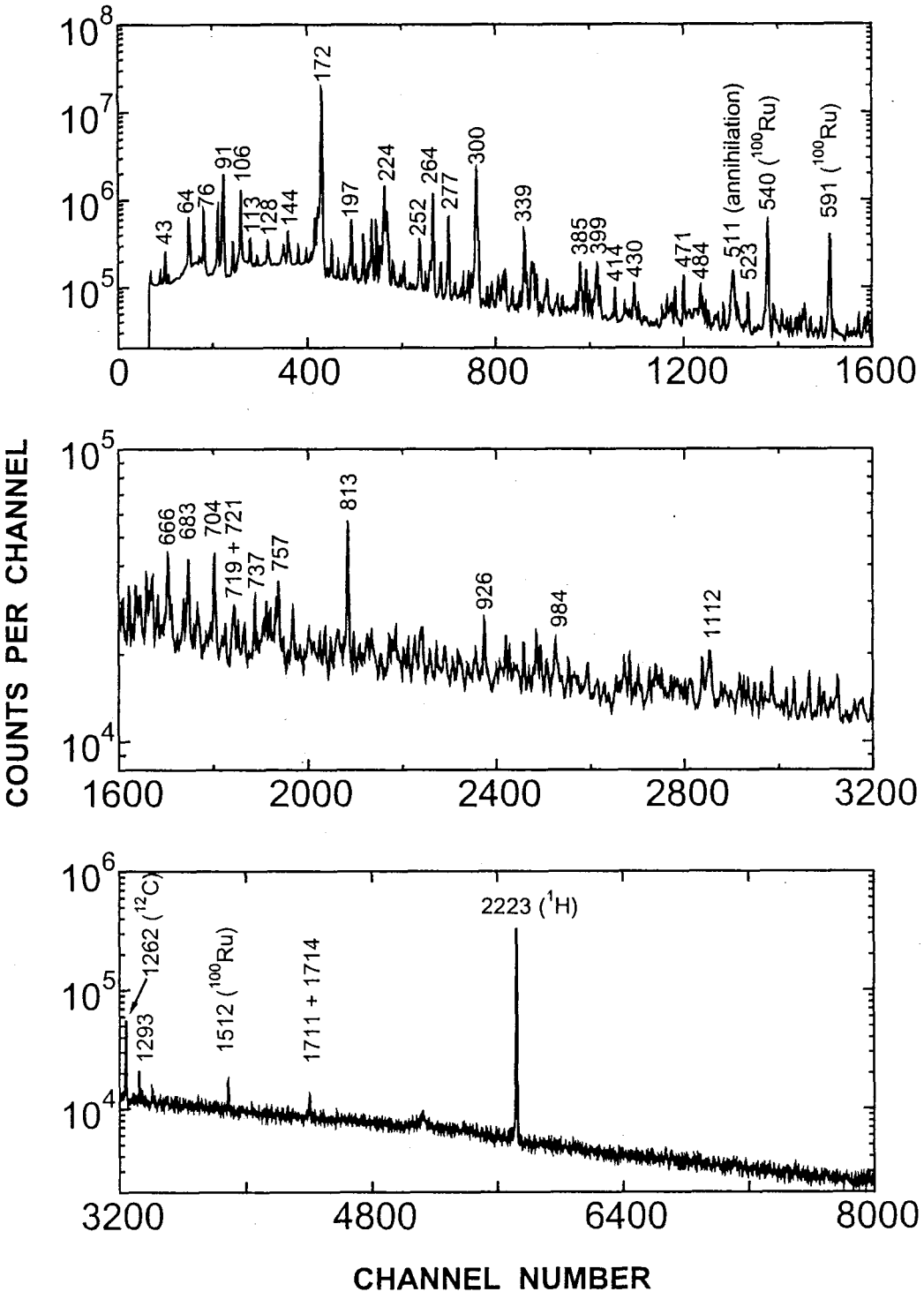

Fig. 2: Gamma-ray spectra from thermal neutron capture by ^{99}Tc. The Ge detector was operated in the Compton-suppression mode. All energies are in keV.

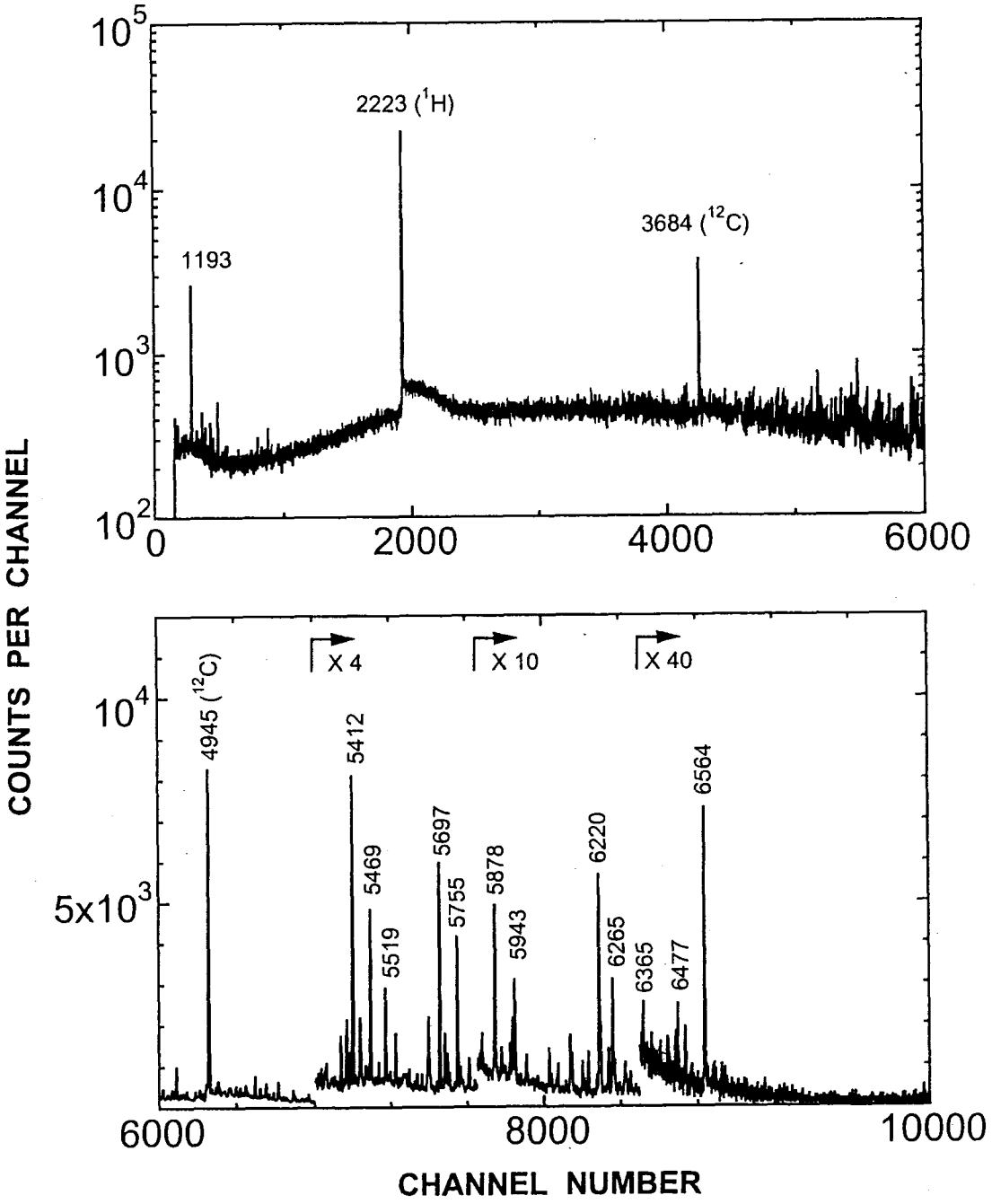

Fig. 3: Gamma-ray spectra from thermal neutron capture by ^{99}Tc. The Ge detector was operated in the pair-spectrometer mode. All energies are in keV.

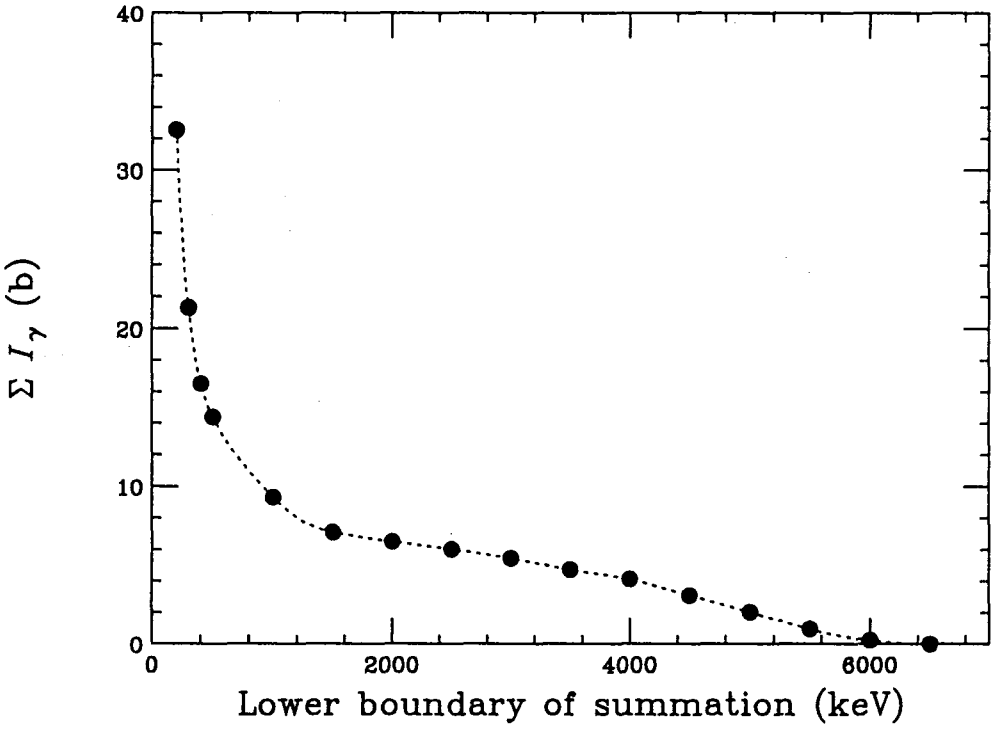

Fig. 4: Sum of gamma-ray cross sections $\sum I_\gamma$ versus the lower limit of the summation.

3 Analysis of prompt γ rays emitted in thermal neutron capture by ^{93}Zr

3.1 Background

The ^{93}Zr nuclide is important in the management of nuclear wastes because of its long half-life as 1.6×10^6(y) [50] and sizable production in fission reactions. As means for reducing the amount of such radioactive fission products, the utilization of neutron capture reactions in a thermal reactor, a fast reactor, and an accelerator-driven reactor have been proposed. To evaluate the transmutation rate in these devices, reliable neutron capture cross sections are needed for the neutron-energy range from thermal and to the MeV region. JNC has been measuring systematically [8, 41, 51–63] the thermal neutron capture cross sections of radioactive fission products and minor actinides using an activation method since 1989. However, the cross section of ^{93}Zr can not be measured via activation because its reaction product ^{94}Zr is stable. At present, the thermal neutron capture cross section of ^{93}Zr is very uncertain. Only two evaluated values for this cross section exist, 2.7±1.4 b [50] and 1.3 b [64].

The aim of this work was to obtain a lower limit for the thermal neutron capture cross section by measuring the emission intensities of prompt gamma rays emitted in the ^{93}Zr($n_{\rm th}$,γ) reaction.

3.2 Experimental procedures

The experimental procedure was the same as that described in the previous chapter. Isotopically enriched ZrO_2 (total weight 114 mg) was used as the sample. The abundance of the Zr isotopes contained in the sample is listed in Table 8.

The experiment was performed in two steps. Firstly, the Zr target was irradiated for about 5 hours together with the 100-mg CH_2 sample to estimate the emission intensity of the prominent gamma rays emitted from the ^{94}Zr. The well-known cross section of the ^{1}H was used for the normalization. Next, only the Zr target was irradiated for about 63 hours to obtain good statistics. Gains of 0.387 keV/ch. in Compton suppressed mode and 1.2603 keV/ch. in pair spectrometer mode were used. Figure 5 show the spectra obtained in Compton suppression mode and in pair spectrometer mode.

3.3 Analyses of measured γ rays

For identification of the gamma rays emitted from ^{94}Zr, information on the known ^{94}Zr levels [64] was utilized. The fifty-two known ^{94}Zr levels are summarized in Table 9. Fifty prompt gamma rays observed in the measurement were assigned to the known levels shown in Table 9.

The 918-keV gamma ray emitted from ^{94}Zr was selected for normalization of emission cross section. From the ratio of the peak intensity of the 918 keV gamma ray to that of 2.225-MeV gamma ray from the ^{1}H(n,γ) reaction measured during the first part of the experiment, the emission intensity was determined. A cross section value of 332.6±0.7 mb was used for the ^{1}H(n,γ) reaction. The emission intensity of the 918 keV gamma ray was deduced as 543 mb.

Next, the spectral data were analyzed which were obtained by the irradiation of the Zr target only. For each gamma ray emitted from ^{94}Zr, the emission intensity was estimated by calculating the ratio of its intensity to that of 918-keV one. The results of the emission intensities are summarized in Table 10. Three gamma rays, at 918-, 1672- and 2847-keV were identified as being due to transitions from excited states to the ground state of ^{94}Zr.

From the values listed in Table 10, summation of the emission intensities of these three gamma rays gives the lower limit of the neutron capture cross section of ^{94}Zr, σ, as

$$\sigma = \sum_{g.s.} I_\gamma = 623.7 \pm 3.9 \text{ mb}.$$

3.4 Discussion

The lower limit of the thermal neutron capture reaction cross section by ^{93}Zr of 623.7±3.9 mb is useful for estimating conditions for future ^{93}Zr cross section measurements.

The energy of capture state was determined to be $S_n(^{94}\text{Zr}) = 8218.1 \pm 0.1$ keV through a least-square fit of level energies to that of γ rays incorporated into the level scheme. The energy of a γ-ray observed at 8217.7 keV was in agreement with that of the capture state within the limits of error. Also, the γ rays observed at 6066, 6160, 6546, 7299 keV can be regarded as primary γ rays because the energies of these γ rays agree with the differences between the energy of the capturing state and known levels. The value of S_n doesn't change after the addition of these five gamma rays. Summing the partial cross sections from these five primary γ leads to a lower limit on the thermal neutron capture cross section of 628.3±3.9 mb.

3.5 Conclusions

In this work, analysis of prompt gamma rays emitted in the thermal neutron capture reaction of ^{93}Zr was performed. As the result of the analysis, four gamma rays, namely 918-, 1672-, 2847-, and 8218-keV gamma rays were identified as ground state transitions. The emission intensities for these gamma-rays were determined relative to the cross section of thermal-neutron

capture reaction by ^{1}H. For the ^{93}Zr(n_{th},γ)^{94}Zr reaction, a lower limit for the thermal neutron capture cross section of 628.3±3.9 mb was obtained.

Table 8: Isotopic abundance of the Zr sample

Mass	Abundance (%)
90	2.29 *5*
91	18.61 *10*
92	18.95 *10*
93	19.98 *10*
94	20.50 *10*
96	19.67 *10*

Table 9: Previously reported energy levels in ^{94}Zr

Level E_γ (keV)	J^π	Excited in which experiment
0.0	0^+	ABCDEFGHIJKLMN
918.75 *5*	2^+	ABCDEFGHIJKLMN
1300.19 *18*	0^+	ABCDEFGKLMN
1469.62 *11*	4^+	ABCDFGIMN
1671.40 *8*	2^+	ABCDFGHIKLMN
2057.64 *10*	3^-	ABCDFGHIMN
2151.31 *20*	2^+	ACDFM
2330.2 *6*	4^+	ACDFI
2366.12 *14*	2^+	ABCDFGIMN
2401 *6*		F
2507.7 *6*	(3^+)	CF
2604.5 *8*	5^-	BCDFGIMN
2698.5 *10*	(1,2,3)	CF
2719		F
2769		F
2826.0 *6*	(2,3)	CF
2846.3 *3*	(1^-)	ACDF
2860.6 *11*	4^+	CFG
2888.2 *17*	4^+	BCDFI
2908.04 *20*	(2^+)	AF
2925 *5*	$(1^-, 3^-, 4^+)$	F
2945.0 *5*	5^-	ABCDI
3014 *8*		B
3030 *6*		F
3059.40 *18*	$1^-, 2, 3, 4+$	ACFI
3156.4 *10*	4^+	BCDFI
3219.43 *13*	3^-	ABCDFGI
3281 *6*	2^+	F
3316 *6*		F
3331 *6*	5^-	DFI
3361.15 *18*	3^-	ABCDFGI
3407 *6*	$(3^-, 4^+)$	FI
3482 *8*		BDFI
3560 *7*	4^+	BFI
3598 *7*	5^-	DFI
3686 *7*		FI
3724.9 *6*	(4^+)	AFI
3776 *7*	0^+	DF

Table 9: (*continued*)

Level E_γ (keV)	J^π	Excited in which experiment
3840 *7*		BFG
3884 *7*		F
3897 *7*	4^+	BDFI
3961.8 *3*	(2^+)	A
4002.2 *15*	$(1, 2^+)$	ABDF
4052.4 *15*	$(1, 2^+)$	A
4081 *8*	(3^-)	FI
4098.5 *15*	$(1, 2^+)$	A
4149 *8*	7^-	FI
4198.8 *4*	$(1, 2^+)$	AD
4225 *8*		DF
4237.6? *5*	$(1, 2, 3)$	A
4340 *8*	4^+	FI
4637.9 *9*	$(1, 2, 3)$	A
4669.8	$(1, 2, 3)^-$	A

A : ^{94}Y β^- decay [65]
B : ^{92}Zr(t,p) [66]
C : ^{94}Zr(n,n'γ) [67]
D : ^{94}Zr(p,p') [68]
E : ^{94}Zr(p,p'γ) [69]
F : ^{94}Zr(d,d') [70]
G : ^{94}Zr(t,t') [71]
H : ^{94}Zr(^{3}He,^{3}He') [72]
I : ^{94}Zr(α,α) [73]
J : Coulomb Excitation [74]
K : ^{94}Mo(^{6}Li,^{8}B) [75]
L : ^{94}Mo(^{14}C,^{16}O) [76]
M : ^{96}Zr(p,t) [77]
N : ^{98}Mo(d,^{6}Li) [78]

Table 10: Energies (E_γ), intensities (I_γ) and placements of the γ rays observed in our ^{93}Zr(n_{th},γ)^{94}Zr measurements

E_γ (keV)	I_γ (mb)	Placement	E_γ (keV)	I_γ (mb)	Placement
309.1 *2*	5.0 *7*	2366→2058	1892.3 *2*	4.8 *7*	3361→1470
381.5 *2*	41.3 *8*	1300→919	1927.2 *2*	5.1 *7*	2846→919
550.9 *2*	92.6 *13*	1470→919	1969.7 *1*	7.0 *6*	2888→919
588.9 *2*	43.0 *9*	2058→1470	2141.0 *1*	12.1 *6*	3059→919
694.8 *1*	16.2 *7*	2366→1671	2237.2 *1*	9.4 *4*	3156→919
752.7 *2*	44.5 *6*	1671→919	2255.3 *2*	3.7 *4*	3725→1470
836.9 *2*	38.7 *8*	2508→1671	2442.4 *2*	3.8 *4*	3361→919
888.1 *3*	10.6 *4*	2945→2058	2492.3 *2*	19.8 *6*	3962→1470
918.8 *2*	543.5 *37*	919→0	2527.9 *3*	2.9 *8*	4199→1671
1001.0 *2*	3.9 *4*	3059→2058	2662.2 *1*	21.0 *6*	3962→919
1066.1 *2*	4.7 *5*	2366→1300	2846.5 *2*	27.1 *7*	2846→0
1134.0 *1*	7.1 *7*	2605→1470	3579.5 *3*	8.5 *14*	C→4638
1139.0 *2*	93.5 *9*	2058→919	4120.5 *2*	10.6 *13*	C→4099
1155.4 *1*	9.2 *4*	2826→1671	4492.6 *2*	10.9 *10*	C→3725
1162.1 *2*	5.6 *14*	3219→2058	5062.1 *3*	6.7 *12*	C→3156
1232.6 *1*	42.3 *7*	2151→919	5158.1 *5*	5.5 *8*	C→3059
1236.4 *2*	6.5 *6*	2908→1671	5309.4 *2*	13.9 *11*	C→2908
1386.4 *2*	3.6 *5*	3059→1671	5371.5 *1*	28.7 *14*	C→2846
1390.9 *1*	7.1 *5*	2861→1470	5711.5 *5*	2.6 *5*	C→2508
1411.1 *1*	18.6 *5*	2330→919	5851.7 *3*	2.6 *4*	C→2366
1447.5 *2*	6.5 *4*	2366→919	6066.4 *2*	7.6 *6*	C→2151
1589.2 *2*	21.2 *6*	2508→919	6159.8 *1*	38.3 *13*	C→2058
1671.5 *2*	53.1 *11*	1671→0	6546.3 *2*	5.7 *8*	C→1671
1750.4 *1*	7.6 *4*	3219→1470	7298.9 *1*	25.1 *9*	C→919
1779.1 *1*	34.1 *8*	2699→919	8217.7 *2*	4.6 *4*	C→0

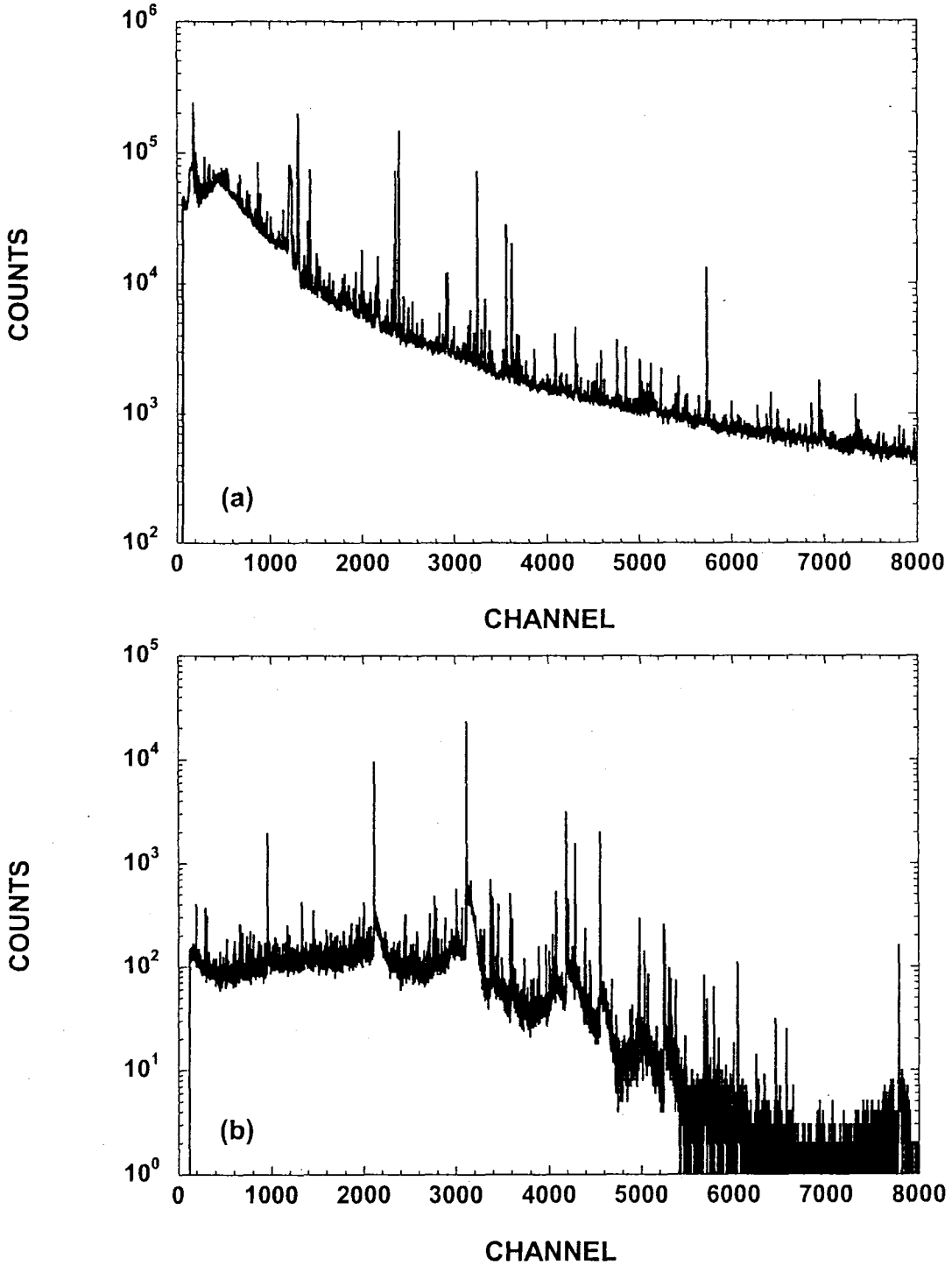

Fig. 5: Spectra of gamma rays emitted in thermal neutron capture reaction by ^{93}Zr obtained in (a) Compton-suppression and (b) pair spectrometer modes. Gains are (a)0.3870keV/ch. and (b)1.2603 keV/ch.

4 Analysis of prompt γ rays emitted in thermal neutron capture by ^{107}Pd

4.1 Background

The ^{107}Pd nuclide is also important in the management of nuclear waste because of its long half-life as 6.5×10^6 (y) [50], so reliable neutron capture cross sections are required.

For the thermal neutron capture cross section by ^{107}Pd, there have been no experimental data reported, but only two *evaluations* [50,64] having identical thermal neutron capture cross sections of 1.8±0.2 b. In addition, a resonance integral of 86.6 b was reported in the evaluation of Ref. [64].

There have been two measurements reported at resonance energies. Macklin [79] measured parameters for 130 resonances up to 3.5 keV. From these, he calculated a capture resonance integral of 108.1±4.3 b, and a 30-keV Maxwell-spectrum average cross section of 1.34±0.06 b. Singh *et al.* [1] measured parameters for 34 resonances below 700 eV. They deduced a capture width Γ_γ for the 6.834 eV resonance of 125±15 meV and estimated the resonance integral to be 87 b. From this limited information, it is very difficult to evaluate the capture cross section for thermal neutrons.

The aim of this work was to obtain a lower limit for the thermal neutron capture cross section of ^{107}Pd through the analysis of the prompt gamma rays emitted from the capture product ^{108}Pd.

4.2 Experimental procedures

The experimental procedures are the same with those described in chapter 2. An isotopically enriched (22.90 %) metal of ^{107}Pd weighing 0.2014 g was used as prepared for the sample. The isotopic composition of the sample

is listed in Table 11. The Pd target was irradiated together with a same 100-mg CH_2 sample so that the ^{107}Pd(n_{th},γ) cross section could be obtained by normalization to the well-known H(n_{th}, γ) one.

Prompt gamma rays emitted from the samples were measured with a Ge detector operated in Compton suppression mode. The gain was 0.40507 keV/ch. The overall measurement time was 87,689 s. An example of gamma-ray spectra is shown in Fig.6.

4.3 Analyses of measured γ rays

Information about the known ^{108}Pd levels [80] was used to identify the gamma ray emitted from the ^{108}Pd sample. The assigned gamma rays are shown in Fig.6. Using this information, 8 gamma rays observed at 434, 931, 1053, 1441, 1540, 2099, 2391, and 2478 keV decay directly to the ground state of ^{108}Pd.

Emission intensities (I_γ) for these γ rays were estimated from the ratios of their peak intensities to that of the 2.225-MeV gamma ray from the ^{1}H(n,γ) reaction. These results are listed in Table 12. By summing the emission intensities for these ground-state transitions, a lower limit of the cross section was obtained as

$$\sum_{g.s.} I_\gamma = 10.2 \pm 0.1 \text{ (b)}.$$

4.4 Discussions

Our lower limit for the thermal neutron capture cross section is about six times larger than the evaluated value. The discussion is made about the evaluated data. The evaluation may be based on the resonance parameters by Singh *et al.* [1] which are listed in Table 13. In the table, the values in the last column were calculated assuming that all resonances are s-wave and

have the same capture width as the 6.834-eV one, namely 125 meV. As a check on this assumption, the thermal neutron capture cross section was then calculated using the following approximate equation,

$$\sigma_0^{\gamma} \approx 4.099 \times 10^6 \left(\frac{A+1}{A}\right)^2 \sum_j^N \frac{g\Gamma_{nj}^0 \Gamma_{\gamma j}}{E_{0j}^2}.$$

With the parameters for 34 resonances listed in Table 13, the thermal neutron capture cross section was calculated to be 1.808 b in agreement with the evaluated one. From this check, the evaluated value might be calculated with some assumption, therefore there is a probability that the thermal neutron capture cross section would increase by taking more resonances into the calculation.

4.5 Conclusions

The prompt gamma rays emitted in thermal neutron capture reaction by the ^{107}Pd were analyzed to obtain a lower limit for the neutron capture cross section of 10.2±0.1 b. This result is about six times larger than the evaluated ones which were estimated by using the known resonance parameters. Such a large value we obtained would suggest the presence of a sub-threshold resonance.

Table 11: Isotopic abundance of the Pd sample

Mass	Abundance (%)
104	1.61 *2*
105	48.50 *5*
106	22.90 *5*
107	15.54 *5*
108	8.77 *2*
110	2.68 *2*

Table 12: Energies (E_γ) and intensities (I_γ) of γ rays from the ^{107}Pd(n,γ)^{108}Pd reaction from our measurement

E_γ (keV)	I_γ (mb)	Placement	E_γ (keV)	I_γ (mb)	Placement
382.3 *6*	10.5 *45*	1314→931	1189.4 *3*	38.6 *53*	1625→434
405.2 *4*	47.9 *85*	1335→931	1233.6 *3*	67.6 *23*	2282→1048
433.1 *5*	7966.7 *758*	434→0	1277.4 *6*	16.1 *61*	2325→1048
496.4 *3*	1928.7 *203*	931→434	1287.3 *3*	39.5 *38*	2218→931
548.0 *3*	38.4 *35*	1990→1441	1351.0 *3*	68.8 *49*	2281→931
607.9 *3*	70.7 *37*	1540→931	1429.2 *3*	50.8 *43*	2478→1048
613.5 *3*	2167.9 *460*	1048→434	1441.3 *3*	214.5 *44*	1441→0
619.1 *3*	102.2 *174*	1053→434	1459.4 *4*	27.2 *40*	2391→931
654.1 *3*	35.5 *26*	1990→1335	1539.7 *3*	103.8 *46*	1540→0
677.5 *3*	43.8 *35*	2218→1540	1554.6 *4*	42.3 *78*	1990→434
693.5 *3*	23.6 *57*	1625→931	1608.9 *4*	39.3 *55*	2540→931
879.5 *3*	93.0 *30*	1314→434	1612.3 *3*	373.9 *141*	2047→434
900.6 *3*	712.6 *74*	1335→434	1664.2 *3*	33.7 *40*	2099→434
908.1 *3*	58.3 *37*	1957→1048	1784.1 *3*	117.4 *65*	2218→434
930.5 *3*	606.4 *61*	931→0	1846.7 *3*	132.6 *49*	2281→434
941.1 *3*	188.4 *44*	1990→1048	1956.2 *3*	45.3 *44*	2391→434
946.4 *3*	194.8 *47*	2282→1335	1969.8 *3*	33.4 *43*	2404→434
998.0 *4*	19.3 *54*	2047→1048	2044.2 *3*	132.8 *69*	2478→434
1006.6 *3*	399.2 *41*	1441→434	2097.5 *3*	82.7 *51*	2099→0
1025.4 *3*	90.6 *29*	1957→931	2106.4 *3*	103.3 *64*	2540→434
1053.1 *3*	863.9 *173*	1053→0	2285.4 *3*	81.5 *75*	2720→434
1057.8 *4*	53.6 *114*	1990→931	2390.7 *3*	263.5 *57*	2391→0
1105.3 *3*	169.2 *76*	1540→434	2477.6 *3*	72.0 *70*	2478→0
1164.6 *4*	53.1 *102*	2218→1053			

Table 13: Resonance parameters for ^{107}Pd [1]

j (No of Res.)	E_{0j} (eV)	$2g\Gamma_{nj}$ (meV)	$\Gamma_{\gamma j}$ (meV)	$g\Gamma^0_{nj}\Gamma_{\gamma j}/E^2_{0j}$
1	3.920	0.0020 *2*		4.1086×10^{-9}
2	5.200	0.023 *2*		2.3313×10^{-8}
3	6.834	0.049 *5*	125 *15*	4.1086×10^{-9}
4	28.00	0.58 *6*		8.7691×10^{-9}
5	41.33	9.62 *60*		5.4883×10^{-8}
6	44.46	35.3 *19*		1.6726×10^{-7}
7	58.94	7.17 *74*		1.6804×10^{-8}
8	73.43	22 *3*		3.0137×10^{-8}
9	84.20	13.1 *13*		1.2959×10^{-8}
10	88.48	26.5 *18*		2.2513×10^{-8}
11	100.6	2.0 *3*		1.2351×10^{-9}
12	114.9	17 *2*		7.5746×10^{-9}
13	132.2	16 *2*		5.0066×10^{-9}
14	140.5	27 *3*		7.2821×10^{-9}
15	152.4	38.1 *36*		8.3151×10^{-9}
16	172.7	125 *20*		1.9929×10^{-8}
17	196.3	4 *1*		4.6226×10^{-10}
18	211.5	2.0 *5*		1.9561×10^{-10}
19	222.9	10 *2*		8.4282×10^{-10}
20	232.6	18 *3*		1.3863×10^{-9}
21	272.0	6.5 *15*		3.2946×10^{-10}
22	292.0	40 *10*		1.6859×10^{-9}
23	301.0	15 *5*		5.9326×10^{-10}
24	325.5	60 *10*		1.9467×10^{-9}
25	369.2	180 *40*		4.3101×10^{-9}
26	376.3	15 *5*		3.3986×10^{-10}
27	380.7	15 *5*		3.3205×10^{-10}
28	472.3	60 *10*		7.8452×10^{-10}
29	489.3	40 *10*		4.6990×10^{-10}
30	538.7	60 *15*		5.5996×10^{-10}
31	559.1	80 *20*		6.7980×10^{-10}
32	587.2	70 *18*		5.2566×10^{-10}
33	628.0	160 *30*		1.0142×10^{-9}
34	654.6	170 *30*		9.6266×10^{-10}

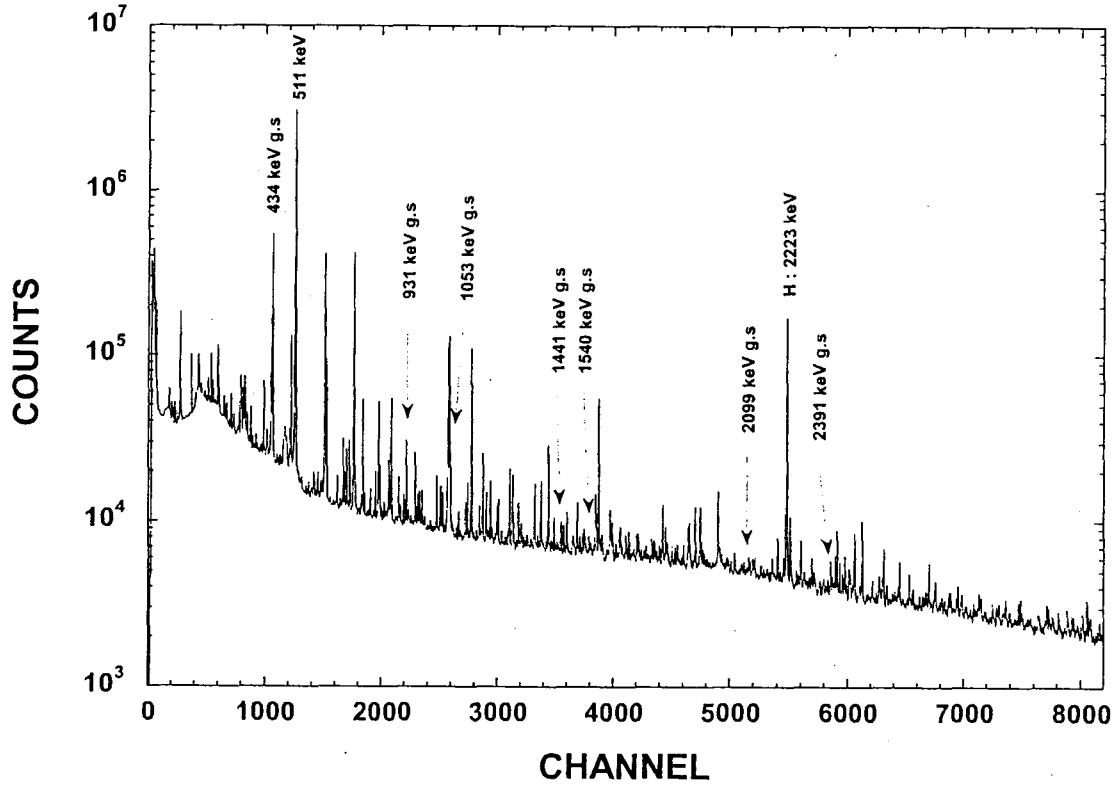

Fig. 6: Gamma-ray spectrum from thermal neutron capture of ^{107}Pd. The Ge detector was operated in Compton suppression mode with a gain of 0.40507 keV/ch.

5 Summary

Previously obtained thermal-neutron capture gamma-ray data were analyzed to deduce the partial neutron-capture cross sections of the LLFPs ^{99}Tc, ^{93}Zr, and ^{107}Pd. By comparing the decay and prompt gamma-ray data for ^{99}Tc, the relation between the neutron-capture cross section deduced by the two different methods was studied. For ^{93}Zr and ^{107}Pd, thermal neutron-capture gamma-ray production cross sections were deduced for the first time. For ^{93}Zr and ^{107}Pd, the lower limits of the capture cross sections for thermal neutron has been deduced for the first time. The level scheme of ^{99}Tc was constructed from the analyzed data and compared with previously reported levels.

6 Acknowledgements

This research was performed as a collaboration between Japan nuclear cycle development institute (JNC) and Oak Ridge National Laboratory (ORNL)(which is operated by UT-Battelle, LLC under the contract No. FERD-01-2094 with the U.S. Dept. of Energy). The other authors dedicate this work to Dr. Subramanian Raman in recognition of his friendship and great contributions to this work and to this field in general.

References

[1] U. N. Singh, et al.: "Neutron Capture and Transmission Measurements on Fission Product Palladium-107", Nucl. Sci. Eng., vol. 67, pp. 54–60 (1978)

[2] S. Raman, et al.: "Thermal neutron capture gamma rays from sulfur Isotopes: Experiment and theory", Phys. Rev. C, vol. 32, no. 1, pp. 18–69 (1985)

[3] R. Firestone: Table of isotopes (1998 Update with CD-ROM), 8th ed., John Wiley & Sons, Inc., New York (1998)

[4] N. J. Pattenden: "Some Neutron Cross Sections of Importance to Reactors Tc^{99}, Nd^{143}, Nd^{145}, Sm^{149}, Sm^{152}, Eu^{151}, Eu^{153}, Gd^{155}, Gd^{157}, Pu^{240}", in Proc. 2nd Int. Conf. Peaceful Uses of Atomic Energy, Geneva, vol. 16, p. 44 (1958)

[5] R. B. Tattersall, et al.: "Pile Oscillator Measurements of Resonance Absorption Integrals", J. Nuclear Energy, vol. 12A, p. 32 (1960)

[6] V. V. Ovechkin, et al.: in Proc. Conf. on Neutron Physics, Kiev 1973, vol. 2, p. 131 (1974)

[7] M. Lucas, et al.: "DETERMINATIONS DES SECTIONS DE CAPTURE NEUTRONIQUE D'ISOTOPES INTERVENANT DANS LE PHENOMENE D'OKLO PAR IRRADIATION DANS LE REACTEUR TRITON", in IAEA-TC-119/14, p. 407 (1977)

[8] H. Harada, et al.: "Measurement of Thermal Neutron Cross Section and Resonance Integral of the Reaction $^{99}Tc(n,\gamma)^{100}Tc$", J. Nucl. Sci. Technol., vol. 32, pp. 395–403 (1995)

[9] J. E. Lynn, et al.: "Analysis of Slow Neutron Capture by ^{9}Be, ^{12}C, and ^{13}C", Phys. Rev. C, vol. 35, no. 1, pp. 26–36 (1987)

[10] S. Kahane, et al.: "Analysis of primary electricdipole gamma rays from slow-neutron capture by Ca isotopes", Phys. Rev. C, vol. 36, no. 2, pp. 533–542 (1987)

[11] S. Raman, et al.: "Thermal-neutron scattering lengths and capture by even calcium isotopes", Phys. Rev. C, vol. 39, no. 4, pp. 1297–1306 (1989)

[12] S. Raman, et al.: "Valence capture mechanism in resonance neutron capture by ^{13}C", Phys. Rev. C, vol. 41, no. 2, pp. 458–471 (1990)

[13] S. Raman, et al.: "Thermal-neutron scattering length and capture by ^{46}Ca", Phys. Rev. C, vol. 44, no. 1, pp. 518–519 (1991)

[14] J. E. Lynn, et al.: "Direct and valence neutron capture by ^{7}Li", Phys. Rev. C, vol. 44, no. 2, pp. 764–773 (1991)

[15] T. A. Walkievicz, et al.: "Thermal-neutron capture by magnesium isotopes", Phys. Rev. C, vol. 45, no. 4, pp. 1597–1608 (1992)

[16] S. Raman, et al.: "Thermal-neutron capture by silicon isotopes", Phys. Rev. C, vol. 46, no. 3, pp. 972–983 (1992)

[17] E. T. Jurney, et al.: "Thermal-neutron capture by ^{14}N", Phys. Rev. C, vol. 56, no. 1, pp. 118–134 (1997)

[18] G. L. Molnár, et al.: "Partial and total thermal neutroncapture cross sections for non-destructive assay and transmutation monitoring of ^{99}Tc", Radiochim. Acta, vol. 90, pp. 479–482 (2002)

[19] A. H. Wapstra: "Energy Calibration for 2-13 MeV Gamma Rays", Nucl. Instrum. Methods Phys. Res., vol. A292, p. 671 (1990)

[20] G. Audi, A. H.Wapstra: "The 1993 Atomic Mass Evaluation. (I). Atomic Mass Table", Nucl. Phys., vol. A565, p. 1 (1993)

[21] S. Raman, et al.: "Efficiency calibration of a Ge detector in the 0.1–11.0 MeV region", Nucl. Instrum. Methods Phys. Res., vol. A454, p. 389 (2000)

[22] D. Cokinos, E. Melkonian: "Measurements of the 2200 m/sec neutron-proton capture cross section", Phys. Rev. C, vol. 15, no. 5, pp. 1636–1642 (1977)

[23] `http://www-rsicc.ornl.gov/codes/psr/psr0/psr-089.html`

[24] M. A. Lone, et al.: "PROMPT GAMMA RAYS FROM THERMAL-NEUTRON CAPTURE", Atomic Data and Nuclear Data Tables, vol. 26, no. 6, pp. 511–559 (1981)

[25] R. C. Reedy, S. C. Frankle: "PROMPT GAMMA RAYS FROM RADIATIVE CAPTURE OF THERMAL NEUTRONS BY ELEMENTS FROM HYDROGEN THROUGH ZINC", Atomic Data and Nuclear Data Tables, vol. 80, no. 1, pp. 1–34 (2002)

[26] P. W.Tarr: "The Experimental Investigation of the Nucleus Technetium-100", Ph.D. thesis, University of Idaho (1972)

[27] D. Heck, J. A. Pinston: "Tables of Gamma-Rays Observed After Thermal Neutron Capture in ^{99}Tc", Internal report KfK2693, Kernforschungszentrum Karlsruhe (1978)

[28] J. A. Pinston, et al.: "Levle structure of ^{100}Tc", Nucl. Phys., vol. A321, pp. 25–44 (1979)

[29] D. N. Slater, W. Booth: "The level structure of ^{100}Tc from a study of the ^{99}Tc(d,p) reaction", Nucl. Phys., vol. A267, pp. 1–12 (1976)

[30] D. J. Martin, S. A. Wender: "Internal conversion in ^{100}Tc", J. Phys. (London), vol. 4, no. 8, pp. 1347–1351 (1978)

[31] Z. Árvay, et al.: "Excited States of ^{100}Tc from ^{100}Mo(p,$n\gamma$)^{100}Tc Reactions and the Parabolic Rule", Z. Phys., vol. A299, pp. 139–147 (1981)

[32] M. Bini, et al.: "Isomeric transitions in ^{100}Tc", Phys. Rev. C, vol. 21, no. 1, pp. 116–123 (1980)

[33] A. M. Bizzeti-Sona, et al.: "Yrast states in the doubly-odd nucleus ^{100}Tc", Z. Phys., vol. A352, pp. 247–255 (1995)

[34] B. Singh: "Nuclear Data Sheets for A = 100", Nuclear Data Sheets, vol. 81, no. 1, p. 1 (1997)

[35] A. H. Wapstra, N. B. Gove: "The 1971 Atomic Mass Evaluation in Five Parts", Nuclear Data Tables, vol. 9, no. 4–5, pp. 265–468 (1971)

[36] D. C. Kocher: "Nuclear Data Sheets for A = 100", Nuclear Data Sheets, vol. 11, p. 279 (1974)

[37] R. S. Hager, E. C. Seltzer: "Internal Conversion Tables. Part I: K-, L-, M-Shell Conversion Coefficients for Z = 30 to Z = 103", Nuclear Data, vol. A4, no. 1 and 2, pp. 1–235 (1968)

[38] `http://www.nndc.bnl.gov/nndcscr/ensdf_pgm/analysis/hsicc/`

[39] O. Dragoun, et al.: "CONTRIBUTION OF OUTER ATOMIC SHELLS TO TOTAL INTERNAL CONVERSION COEFFICIENTS", Nuclear Data Tables, vol. A9, pp. 119–135 (1971)

[40] Z. Németh, A. Veres: "COMPARISON OF EXPERIMENTAL AND THEORETICAL HIGH MULTIPOLE-ORDER INTERNAL CONVERSION COEFFICIENTS", Nucl. Instrum. Methods Phys. Res., vol. A286, pp. 601–606 (1990)

[41] K. Furutaka, et al.: "Precise Measurement of Gamma-Ray Emission Probabilities of ^{100}Ru", J. Nucl. Sci. Technol., vol. 38, pp. 1035–1042 (2001)

[42] R. B. Tattersall, et al.: J. Nuclear Energy, vol. 12A, p. 16 (1960)

[43] H. Pomerance: "Thermal absorption cross section of ^{99}Tc", Tech. Rep. ORNL-1975, 31, 5509, Oak Ridge National Laboratory (1975)

[44] P. F. Rose: "ENDF-201, ENDF/B-VI summary documentation", Tech. Rep. BNL-NCS-17541, 4th ed., Brookhaven National Laboratory (1991)

[45] T. Nakagawa, et al.: "Japanese Evaluated Nuclear Data Library Version 3 Revision-2: JENDL-3.2", J. Nucl. Sci. Technol., vol. 32, p. 1259 (1995)

[46] K. Shibata, et al.: "Japanese Evaluated Nuclear Data Library Version 3 Revision-3: JENDL-3.3", J. Nucl. Sci. Technol., vol. 39, p. 1125 (2002)

[47] H. Bartsch, et al.: "An Investigation of short-lived Isomers in the Nuclei ^{90,92}Nb, ^{99}Mo, ^{98,100,101}Tc and ^{101}Ru", Z. Phys., vol. A285, pp. 273–281 (1978)

[48] R. L. Macklin: "Technetium-99 Neutron Capture Cross Section", Nucl. Sci. Eng., vol. 81, p. 520 (1982)

[49] H. Akimune, et al.: "GT strengths studied by (^{3}He,t) reactions and nuclear matrix elements for double beta decays", vol. 394, pp. 23–28 (1997)

[50] R. B. Firestone: Table of Isotopes, 8th ed., John Wiley & Sons, Inc., New York (1996)

[51] H. Harada, et al.: "Measurement of Thermal Neutron Cross Section of ^{137}Cs(n,γ)^{138}Cs Reaction", J. Nucl. Sci. Technol., vol. 27, p. 577 (1990)

[52] T. Sekine, et al.: "Measurement of Thermal Neutron Cross Section and Resonance Integral of the Reaction ^{137}Cs(n,γ)^{138}Cs", J. Nucl. Sci. Technol., vol. 30, p. 1099 (1993)

[53] S. Nakamura, et al.: "Measurement of Thermal Neutron Capture Cross Section and Resonance Integral of the $^{129}I(n,\gamma)^{130}I$ Reaction", J. Nucl. Sci. Technol., vol. 33, p. 283 (1996)

[54] T. Katoh, et al.: "Measurement of Thermal Neutron Cross Section and Resonance Integral of the Reaction $^{135}Cs(n,\gamma)^{136}Cs$", J. Nucl. Sci. Technol., vol. 34, p. 431 (1997)

[55] Y. Hatsukawa, et al.: "Thermal Neutron Cross Section adn Resonance Integral of the Reaction of $^{135}Cs(n,\gamma)^{136}Cs$: Fundamental data for the transmutation of nuclear waste", J. Radioanal. Nucl. Chem., vol. 239, p. 455 (1999)

[56] T. Katoh, et al.: "Measurement of Thermal Neutron Capture Cross Section and Resonance Integral of the Reaction $^{127}I(n,\gamma)^{128}I$", J. Nucl. Sci. Technol., vol. 36, p. 223 (1999)

[57] S. Nakamura, et al.: "Measurement of Thermal Neutron Capture Cross Section and Resonance Integral of the Reaction $^{133}Cs(n,\gamma)^{134m,134g}Cs$", J. Nucl. Sci. Technol., vol. 36, p. 847 (1999)

[58] H. Harada, et al.: "Measurement of Effective Neutron Capture Cross Section of ^{166m}Ho using Two Step Irradiation Technique", J. Nucl. Sci. Technol., vol. 37, no. 9, pp. 821–823 (2000)

[59] H. Wada, et al.: "Production of the Isomeric State of ^{138}Cs in the Thermal Neutron Capture Reaction $^{137}Cs(n,\gamma)^{138}Cs$", J. Nucl. Sci. Technol., vol. 37, no. 10, pp. 827–831 (2000)

[60] S. Nakamura, et al.: "Measurement of the Thermal Neutron Capture Cross Section and the Resonance Integral of the $^{90}Sr(n,\gamma)^{91}Sr$ Rection", J. Nucl. Sci. Technol., vol. 38, p. 1029 (2001)

[61] T. Katoh, et al.: "Measurement of Thermal Neutron Capture Cross Section and Resonance Integral of the $^{166m}Ho(n,\gamma)^{167}Ho$ Rection using a Two-Step Irradiation Technique", J. Nucl. Sci. Technol., vol. 39, p. 705 (2002)

[62] T. Katoh, et al.: "Measurement of Thermal Neutron Capture Cross Section and Resonance Integral of the $^{237}Np(n,\gamma)^{238}Np$ Reaction", J. Nucl. Sci. Technol., vol. 40, no. 8, pp. 559–568 (2003)

[63] S. Nakamura, et al.: "Measurement of the Thermal Neutron Capture Cross Section and the Resonance Integral of the $^{109}Ag(n,\gamma)^{110m}Ag$", J. Nucl. Sci. Technol., vol. 40, p. 119 (2003)

[64] http://www.nndc.bnl.gov/nndc/ensdf/

[65] B. Singh, et al.: "A study ofthe gamma radiation from the decay of ^{94}Y", J. Phys. (London), vol. G2, no. 6, p. 397 (1976)

[66] E. R. Flynn, et al.: "The (t,p) reaction to the low-lying levels of the zirconium isotopes", Nucl. Phys., vol. A218, p. 285 (1974)

[67] G. P. Glasgow, et al.: "Level and decay scheme studies in ^{92}Zr and ^{94}Zr", Phys. Rev. C, vol. 18, no. 6, pp. 2520–2546 (1978)

[68] J. K. Dicens, et al.: "^{90,92,94}Zr(p,p') Reactions at 12.7 MeV", Phys. Rev., vol. 168, pp. 1355–1372 (1968)

[69] S. Cochavi, et al.: "Mean Lifetime of the Second 0^+ States in ^{92}Zr and ^{94}Zr", Phys. Rev. C, vol. 1, no. 5, pp. 1821–1825 (1970)

[70] R. K. Jolly, et al.: "Studies of 15-MeV Inelastic Deuteron Scattering", Phys. Rev., vol. 128, no. 5, pp. 2292–2302 (1962)

[71] E. R. Flynn, et al.: "Inelastic Triton Scattering from ^{92,94,96}Zr", Phys. Rev. C, vol. 1, no. 2, pp. 703–713 (1970)

[72] D. E. Rundquist, et al.: "^{3}He Scattering from Nickel and Zirconium Isotopes", Phys. Rev., vol. 168, no. 4, pp. 1287–1295 (1968)

[73] P. Singh, et al.: "Alpha scattering from ^{92}Zr and ^{94}Zr", Nucl. Phys., vol. A458, pp. 1–11 (1986)

[74] M. Hass, et al.: "Magnetic moments of the 2_1^+ levels in ^{92}Zr and ^{94}Zr", Phys. Rev. C, vol. 22, no. 3, pp. 1065–1067 (1980)

[75] R. S. Tickle, et al.: "Two-proton pickup in the zirconium region using the (^{6}Li, ^{8}B) reaction", Nucl. Phys., vol. A376, pp. 309–324 (1982)

[76] W. Mayer, et al.: "Strong population of excited 0^+ states in even Zr isotopes observed with the (^{14}C, ^{16}O) reaction", Phys. Rev. C, vol. 26, no. 2, pp. 500–510 (1982)

[77] J. B. Ball, et al.: "Study of the Zirconium Isotopes with the (p,t) Reaction", Phys. Rev. C, vol. 4, no. 1, pp. 196–214 (1971)

[78] A. Saha, et al.: "Unusually strong excitation of the 1.59 MeV 0^+ state in the ^{100}Mo(d,^{6}Li)^{96}Zr reaction", Phys. Lett., vol. 82B, no. 2, pp. 208–211 (1979)

[79] R. L. Macklin: "Neutron Capture Measurements on Fission Product ^{107}Pd", Nucl. Sci. Eng., vol. 89, pp. 79–86 (1985)

[80] http://www.nndc.bnl.gov/nndc/nudat/